AD NUMBER: AD0391707
CLASSIFICATION CHANGES
TO: Unclassified
FROM: Confidential
LIMITATION CHANGES
TO: Approved for public release; distribution is unlimited.
FROM: Distribution authorized to U.S. Gov't. agencies and their contractors; Administrative/Operational Use; 31 DEC 1960. Other requests shall be referred to Office of Naval Research, Arlington, VA 22203.
AUTHORITY
U per ONR ltr dtd 1 Nov 1968; ST-A per ONR notice dtd 27 Jul 1971

INVESTIGATIONS ON THE DIRECT CONVERSION OF NUCLEAR FISSION ENERGY TO ELECTRICAL ENERGY IN A PLASMA DIODE (U)

FINAL REPORT NO. 8

VOLUME II

OFFICE OF NAVAL RESEARCH

Contract Nonr-3109(00)

JUNE 28, 1968

Research Laboratories, General Motors Corporation

Warren, Michigan 48090

RESTRICTED DATA

This document contains restricted data as defined in the Atomic Energy Act of 1954. Its transmittal or the disclosure of its contents in any manner to an unauthorized person is prohibited.

Research Laboratories

NOTICE

This document has been withdrawn from the DDC bulk storage. It is the responsibility of the recipient to promptly mark it to indicate the reclassification action shown hereon.

General Motors Corporation

(14) GMR-[redacted]-2731

Copy # 26

OFFICE OF NAVAL RESEARCH

Contract Nonr-3109(00)

(15)

(16) NR-099-345

(6) Investigations on the Direct Conversion of Nuclear Fission Energy to Electrical Energy in a Plasma Diode, (U)

Final Report No. 8 (8)

VOLUME II

(9) Rept. no. 8 (Final), 1 Nov 66-31 Oct 67,

(10) Authors

Fay E. Gifford,

Charles B. Leffert

David B. Rees

Frank E. Jamerson

Frank E. Jamerson
Project Supervisor

(11) 28 Jun 68

(12) 61p.

Report for Period 1 November 1966 to 31 October 1967
Report Published 28 June 1968

Research Laboratories, General Motors Corporation

Warren, Michigan

150-500

1473

This report has been prepared under Contract Nonr-3109(00) for the Office of Naval Research and technically supervised by Commander Ollie Loper, Commander William F. Diehl and Dr. Ralph Roberts.

ABSTRACT

This is the classified section (Vol. II) of the Final Report under Contract Nonr-3109(00), Office of Naval Research, dealing with fission-fragment-generated plasmas for thermionic energy conversion. Inpile experiments on the transport of thermionic electrons through the argon-cesium plasma are described and the results are compared with predictions of a diffusion-loss dominated transport model and recombination-dominated limits. The inpile experiments were performed using ceramic-metal diodes of parallel-plane configuration, filled to a pressure $p(Ar) \approx$ about 100 torr and $10^{-6} \lesssim Cs/Ar \lesssim 10^{-2}$, with an unclad thermionic-electron and fission-fragment emitter, ($BaO\text{-}UO_2\text{-}W$), and also containing an evacuated electron-gun section by means of which the emitter temperature could be heated in a manner independent of the nuclear heat. Maximum short-circuit current densities of about 0.3 A/sq cm were obtained in these diagnostic diodes at a neutron flux value of around 1×10^{13} cm^{-2} sec^{-1}. These current densities were much higher (by factors of 5 to 30) than those predicted by the diffusion-loss dominated transport-model. Furthermore, in marked contrast with theory, these current densities were similar for two values of emitter-collector spacing (0.15 and 0.3 cm). This makes the present system appear more attractive for practical thermionic applications than can be expected on the basis of simple transport-models. Quantitative recombination-dominated limits suggest that the experimental findings are more consistent with a uniform emitter-collector electron density profile. As a result, it is tentatively suggested that the incidence of excited and charged argon species upon cesium-covered metal surfaces gives rise to a wall source of both ions and electrons which in effect significantly reduces the expected ambipolar diffusion loss of charge from the plasma.

CRD *

---

* Each component of this report is labeled in the right margin with abbreviations (U=Unclassified, C=Confidential, RD=Restricted Data) according to the U.S. AEC "Classification Guide for Thermionic Converters", CG RTC-2 (Oct., 1964).

Ten trillion per sq cm per sec.

CONTENTS

U

LIST OF FIGURES

Figure

U

OBJECTIVES

The objectives of the classified studies for the current reporting period were to operate several inpile thermionic electron transport diodes with appropriate Ar-Cs fillings, and extend the theoretical transport studies to include reaction kinetic results, with the purpose of understanding electron transport sufficiently well to enable us to extrapolate the results to a power reactor and thus assess the utility of fission-fragment-generated plasmas in a nuclear thermionic converter. U

CONCLUSIONS

Many general conclusions relevant to the present study and overall program are of an unclassified nature and are discussed fully in Vol. I. The following are the more detailed conclusions from the inpile electron transport work reported in this classified Vol. II. U

(i) The maximum inpile short-circuit currents through the Ar-Cs electron transport tubes were obtained for the seeding range of $10^{-2} \lesssim Cs/Ar \lesssim 10^{-6}$ over which the currents were generally insensitive to Cs/Ar ratio. The fact that very small Cs/Ar ratios ($\sim 10^{-6}$) could yield maximum current values is consistent with earlier microwave data which indicated that the measured electron density in microwave cavities remained at near-peak values as the Cs/Ar ratio was changed from about 10^{-4} to 10^{-6}. CRD

(ii) Short circuit current densities of about 0.3 A cm^{-2} at values of neutron flux$\sim 1 \times 10^{13} cm^{-2} sec^{-1}$ were much higher (by factors of 5 to 30) than those expected from a diffusion-loss dominated transport model. Again these high currents were in line with an extrapolation to high temperature of some of the unexplained argon-cesium microwave data of electron density versus gas temperature. CRD

(iii) The same value of maximum inpile short circuit current (0.9 A) was obtained with two diodes which in essence differed only in gap spacing, viz., diode No. 2 had a gap of 0.3 cm, whereas diode No. 4 had a gap of 0.15 cm. This result is incompatible with the expected dominance of ambipolar diffusion as the charge loss mechanism. It is in accord with a more uniform emitter-collector electron density distribution. CRD

(iv) We conclude that there exists significant consistency in the experimental microwave and transport data on Ar-Cs to lend considerable weight to the validity of the two sets of data. However, we have not been able to account theoretically for the higher values of electron density and transport current despite much searching in the areas of temperature-dependent reaction rates, heteronuclear ions and thermal surface ionization. A diagnostic diode to investigate the anomalously high electron transport was designed and built but this final tube failed prior to insertion in the reactor. We indicate that the results are consistent with the idea that the incidence of excited and charged argon species upon cesium-covered metal surfaces gives rise to a wall source of both ions and electrons. In the absence of a quantitative explanation it is not possible to extrapolate the present data to a thermionic converter in a power reactor, i.e., a definitive statement regarding the utility of the fission fragment scheme cannot be made without further study. It can be stated, however, that the present system is much more attractive for thermionic converter applications than expected on the basis of a simple diffusion-loss dominated transport model. U

I. INTRODUCTION

In the unclassified Volume I of this Final Report, we presented a summary of our previcus unclassified work performed under Contract Nonr-3109(00), Office of Naval Research.[1-7] That summary described the results of our theories and experiments on ion generation rates by fission fragments and electron densities in single, mixed and cesium-seeded noble gases. Those studies, U conducted in the absence of thermionic emission, were considered necessary to elucidate many of the basic mechanisms of ion production and reaction kinetics in these somewhat unique and quiescent plasmas. The next step in assessing the fission-fragment-ionization scheme for thermionic energy conversion applications was to mate the most suitable gas filling with an appropriate thermionic emitter. This last phase of our program – thermionic electron transport – is the subject of the present classified Volume II.

We concluded from our unclassified studies that the most suitable gas filling for our electron transport tubes was argon-cesium with an argon density $[Ar] \approx 3\times10^{18}\,cm^{-3}$ and a low cesium seeding, viz., $[Cs]/[Ar] \lesssim 10^{-4}$. U Briefly, argon has an exceedingly low Ramsauer minimum (i.e. low resistance to electron flow) at the right energy point ($\sim$0.2 eV) for a converter, argon metastables have a very large cross section ($\approx 10^{-14}\,cm^{-2}$) for ionizing neutral cesium which in turn leads to high electron densities, and a cesium covering can be used on the collector to yield a low work function surface. More detailed reasons for this choice of gas filling and density are fully outlined in Section I of Volume I where we also point out from calculations and inpile microwave measurements that single and binary mixtures of noble gases are not promising for practical thermionic energy conversion applications involving fission fragment ionization. Consequently, our experiments and calculations of electron transport have been concentrated on the argon-cesium system. In addition, we selected spacings of about 1 mm for the transport diodes. This spacing appeared appropriate from our reaction kinetics studies of electron densities, and also, from an electron transport standpoint, such relatively large spacings are potentially feasible because of the low argon electron scattering cross section.

The thermionic-electron and fission-fragment emitter used in the electron transport tubes was an unclad $BaO\text{-}UO_2$-W cermet designed to operate at

a temperature of 1400°C with current density capability of about 10 A cm^{-2}. This emitter was originally developed under Contract Nonr-3870(00), Office of Naval Research and was fully described in Part I (unclassified) and Part II (classified) of the Final Report, July 1, 1964. The fission fragment flux (and hence gas ionization rate) from the BaO-UO_2-W emitter is significantly lower (by factors of 4 to 8) than that from the 1 mil-thick U-235 foils used in our previous unclassified studies. This arises not only from the presence in the thermionic emitter of non-fissionable materials necessary for good thermionic-electron emission; equally as important is the fact that the BaO-UO_2-W emitter has to be relatively thick to yield the high temperature for thermionic emission, and this very thickness leads to significant neutron attenuation which depresses the neutron flux at the emitter surface and thus reduces the fission fragment flow from the emitter into the gas. In contrast, a 1-mil thick U-235 foil is largely transparent to neutrons and so does not significantly depress the neutron flux at the fission-fragment-emitting surface. With this in mind, we note that the first four electron transport tubes (ETT 1-4) were designed with a BaO-UO_2-W emitter and a molybdenum collector whereas the final electron transport tube (ETT-5) contained a U-235 foil on the collector surface and a pure thermionic electron surface, viz., a Philips cathode, as the emitter. This latter diagnostic device was thus designed to have a higher fission-fragment ionization rate and lower emitter temperature (10 A cm^{-2} at 1100°C) than diodes ETT 1-4. U

The diodes discussed in this report were not designed to be efficient thermionic energy converters since no attempt was made at this time to incorporate a low work function collector and optimize output power. The diodes are termed electron transport tubes because they were designed to study the transport of thermionic electron current through the fission-fragment-generated plasma. Our earlier inpile microwave cavities (with no thermionic current) were operated, for fabrication reasons, only at gas temperatures $\lesssim$ 700°C and so it was also of particular interest to extend this temperature up to a range (1400°C) more in accord with the operating temperature of a practical thermionic device. Our goal has been to incorporate the salient ion production and loss mechanisms from our well-proven reaction kinetics theories into an electron transport model which would be capable of predicting the current-voltage U

characteristics of the electron transport tubes operating inpile under a variety of conditions. As discussed in the subsequent sections, this goal has not been realized. Nevertheless, by comparing the inpile electron transport tube data with predictions of a diffusion-dominated electron transport-theory and recombination-dominated limits, certain definitive conclusions can be made. Interestingly, we find that the incidence of excited and charged argon species upon a cesium-covered surface appears tantamount to neglecting ambipolar diffusion loss from the system. U

II. SYNOPSIS OF EXPERIMENTAL HARDWARE

Three electron transport tubes (ETT) were operated in the University of Michigan Phoenix Memorial Reactor (swimming-pool type, 2 megawatt maximum power). U The tubes were basically ceramic-metal planar diodes operated at temperatures as high as 1400°C and filled with both argon at pressures of about 100 torr and trace amounts of cesium. The diodes were contained in a 4 ft long, 3 in. o.d. evacuated aluminum tube positioned in the reflector region of the reactor. A 20 ft long, 1.5 in. o.d. aluminum tube was attached to one end of the 4 ft tube to provide mechanical support and contained the electrical leads and coolant plumbing to the diodes. The neutron flux measured at the emitter position (gold foil activation, emitter absent) gave a value of 9×10^{12} $cm^{-2} sec^{-1}$ when extrapolated to full reactor power of 2 MW.*

The data were taken in the form of current-voltage plots of the diode output; the collector voltage was swept through a range of positive and negative values to include both the forward and back saturated output currents (+3V to -10V was usually sufficient). The temperatures of the electrodes, diode envelope and other components were measured by recording the output of thermocouples on a 16 point strip chart recorder. U

The first diode (No. 1) was fabricated to check the basic design and construction; the next three diodes (Nos. 2, 3 and 4) had a $BaO\text{-}UO_2\text{-}W$ emitter designed to operate inpile at 1400°C while the last (No. 5) had a Philips cathode emitter designed to operate at 1100°C. The collectors were all made of molybdenum except for the last diode which had a collector consisting of uranium brazed onto molybdenum. The emitters were separated from the collectors by two ceramic insulators which isolated a guard ring in between. The guard ring facilitated the electronic measurements. Figure 1 shows the design of the electron transport tube. Much of the construction techniques involved in diodes ETT-2, 3 and 4 have been described in a previous report.[2] Special attention is given to the fabrication of ETT-5 at the end of the next section (II-1). U

The temperature of the emitters could be varied by three methods, viz: (1) by changing the power of the reactor ($\leq$ 2 MW); (2) by mechanically moving the tube in or out of the reactor core; or (3) by applying auxiliary electronic power to the electron gun incorporated in the tube (see Fig. 1). U

* We generally quote the unperturbed neutron flux (as measured by our flux probe) and this value at the core centerline is typically 1.4×10^{13} $cm^{-2} sec^{-1}$ at full reactor power.

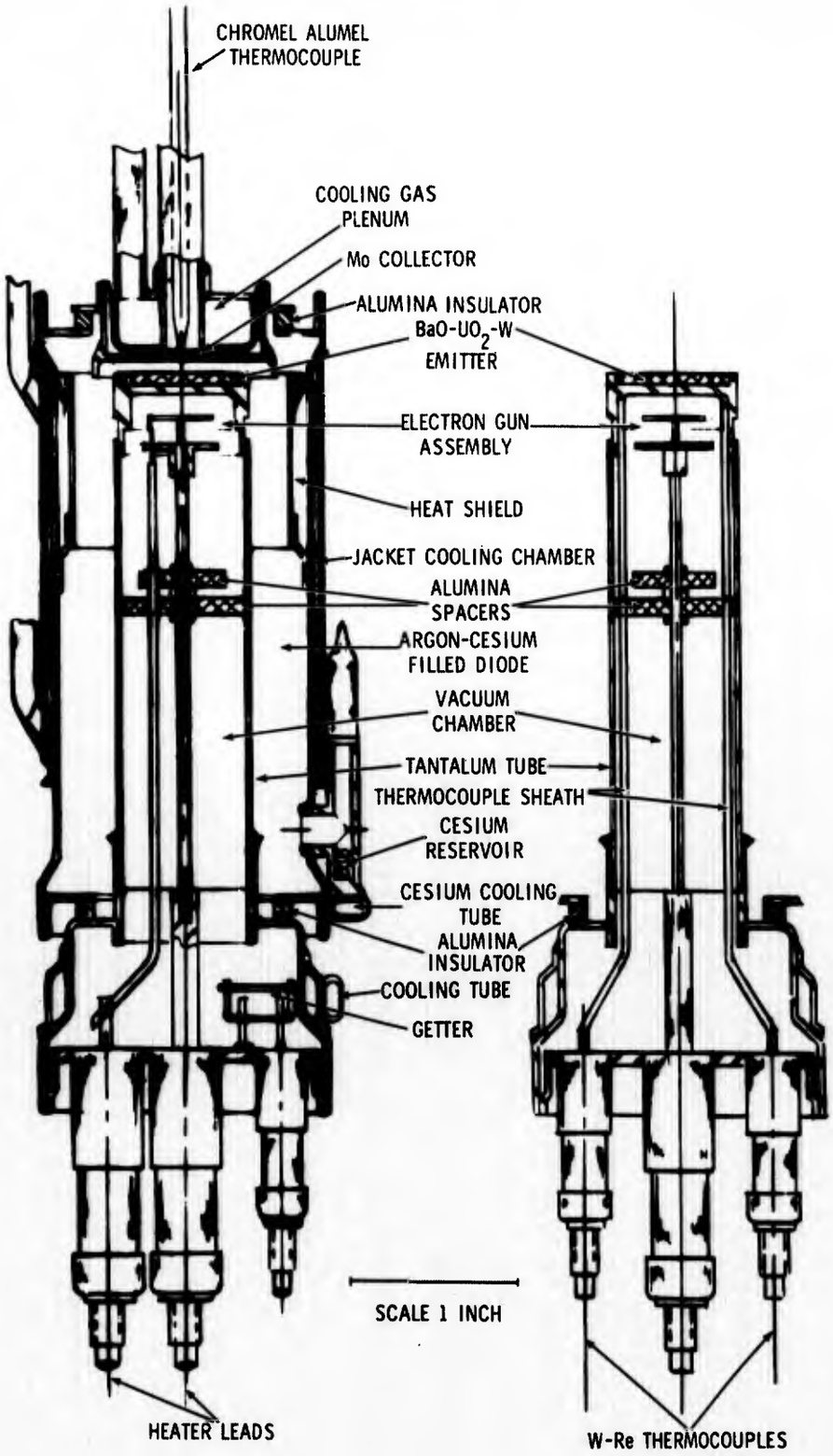

CRD

Fig. 1. Design of electron transport tube.

In general, sufficient cooling for the electron gun, guard ring and collector was obtained by recirculating nitrogen gas through the respective plenums shown in Fig. 1. Increased cooling from helium gas was tried in diode 4 in an effort to determine the effect of collector temperature on the back electron emission from the collector. U

Diodes 2 and 3 were examined in the hot cell after operation in the CRD reactor to determine the cause of failure and, subsequently, to modify succeeding diodes if there was a mechanical or electrical weakness. Diode 2 failed because the collector thermocouple had pulled away from the back side of the collector face and therefore indicated too low a temperature. As a consequence the braze joint holding the collector to the coolant plenum melted and this allowed the radioactive gases in the diode to mix with the nitrogen cooling gas. Diode 3 never reached the designed operating temperature of 1400°C; consequently the inpile experiments were terminated after only 8 hours. It was learned in the hot cell that diode 3 had insufficient emitter-core thickness to reach 1400°C inpile. With diode 4, a water leak developed in the 4 ft aluminum containment tube. A 1 in. thick Delrin plate that sealed the top end of the 4 ft tube developed small cracks after exposure to the neutron flux for 50 megawatt hours. Diode 5 developed a leak in the copper tube pinch-off region within a few days after pinch-off, prior to any reactor tests.

A few days after seal-off (just prior to going into the reactor), the full output power of the electron guns in diodes 2, 3 and 4 could no longer be realized. Arcing occurred when high voltage was applied between the heater and emitter. A 5 mg barium "Kic" getter was incorporated in each evacuated gun section of the diodes but it is conjectured that this did not provide sufficient getter action for the amount of gas or type of gas evolved. However, the electron-gun heaters in diodes 3 and 4 continued to operate through most of the tests in the reactor. The heater alone supplied about one-half the desired power, viz. 100 watts. A 2 in. length by 0.010 in. diameter wire alloy (25% titanium - 75% tantalum) wound on a 0.125 in. mandrel served as the getter in diode 5, and this entire gun was operative throughout all the laboratory tests. U

II. 1. Fabrication

A total of five electron transport tubes were fabricated. The latter four were filled with Cs and argon for performance tests whereas the first tube (ETT-1) was fabricated to obtain necessary design information for the subsequent U

diodes. This design information included: (1) power required to attain the desired emitter temperatures; (2) electron gun design; (3) operating temperatures of the major components in the diode (see Fig. 2); (4) allowance in the emitter-collecting spacing for thermal expansion of the tantalum tube supporting the emitter; and (5) brazing and heliarc techniques. Subsequent discussion pertains only to the last four tubes designed for the reactor.

Three of the four diodes (ETT-2, 3 and 4) contained an uranium bearing emitter. The last diode (ETT-5) had a Philips cathode emitter. Emitters which would operate at 1400°C were selected for ETT-2, 3 and 4 since this temperature was sufficiently high to expect reasonable emission without causing undue stresses on seals and materials. The emitter temperature selected for ETT-5 was 1100°C. Table I lists pertinent differences between the diodes. The argon filling pressure shown in the table is the argon pressure at 300°K to which the cold electron transport tubes were filled. Under operating conditions, the temperature distribution throughout the diode (cf. Fig. 2) is such that the atomic number density in the hot emitter-collector region is

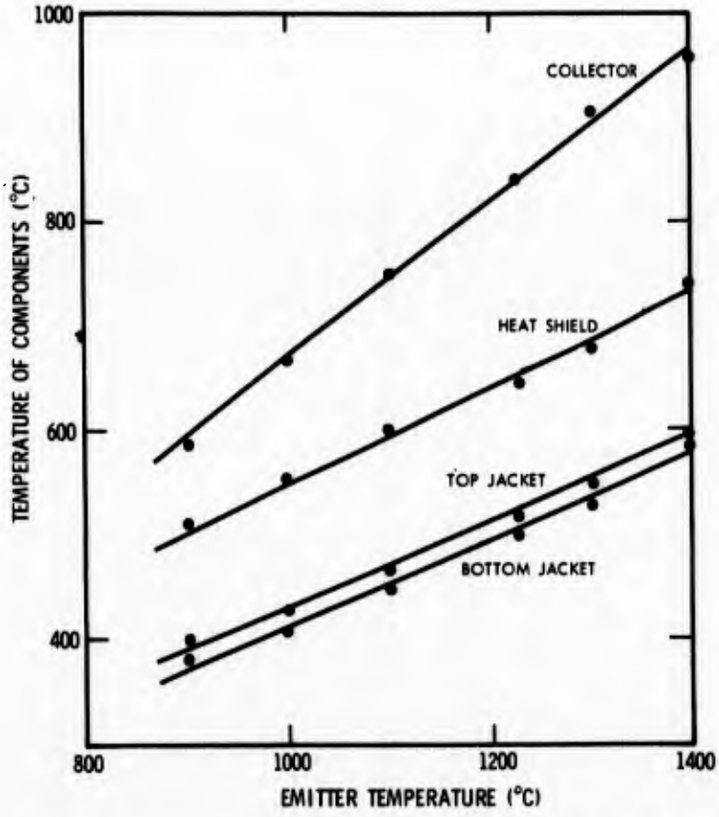

Fig. 2. Temperature distribution of major components of tube shown in Fig. 1.

reduced to about 3×10^{18} cm^{-3} (equivalent to about 100 torr at 300°C). The actual value of the $[Cs]/[Ar]$ ratio in the emitter-collector region is carefully calculated in each case from the initial argon filling pressure, the temperature distribution throughout the diode, and the temperature of the cesium reservoir.

Battelle Memorial Institute fabricated a total of 13 enriched, 0.750 in. U diameter, $BaO\text{-}UO_2$-W emitters for the program. Three of these were built into transport tubes; four were destructively analyzed by BMI; three were destructively analyzed by GMR; one had a damaged tantalum support tube, and two are in vacuum storage.

TABLE I. Pertinent differences between diodes. CRD

Tube No.	Type of Emitter	Collector Material	Interelectrode Spacing (mils)	Argon Filling Pressure (torr)	T_E (°C)
ETT-2	E-7645	Mo	125	150	1400
ETT-3	E-7638	Mo	62	150	1400
ETT-4	E-7552	Mo	62	130	1400
ETT-5	Philips	U on Mo	62	120	1100

The various emitter compositions are identified by a four number system U which is a code to their composition. The first two numbers indicate the volume percent loading of oxide in the emitter while the last two numbers indicate the mole percent barium oxide in the oxide portion. For example, a number 7645 would indicate 76 v/o oxide (24 v/o tungsten) with the oxide portion containing 45 m/o BaO (55 m/o UO_2).

Table II lists these emitters along with information on their weight, thickness, thermionic emission capability at 1400°C and radioactive α-counts per minute. High values of α-count are desirable since this indicates a high uranium coverage on the emitter surface to provide a high fission-fragment flux. High thermionic currents and α-counts are not, however, sufficient properties for a suitable $BaO\text{-}UO_2$-W emitter; there must also be enough fissionable uranium present to heat the emitter to the required temperature of 1400°C. This latter requirement is discussed further in the next section (II.2). In addition to the enriched emitters, six natural emitters were fabricated as laboratory samples for emission, evaporation compatibility and technique studies. There were 3 each of compositions 7552 and 7638 fabricated.

TABLE II. Emitters fabricated for tests and diode operation. CRD

Item	Emitter (Enriched)	α (c/m as received)	Current (Amp at 1400°C)	Core Thickness (mils)	Electron Transport Tube No.
(1)	7645-D	640,700	> 7.5	41	2
(2)	7552-E	346,900	> 8.0	–	
(3)	7552-F	346,700	0.3	–	
(4)	7645-G	570,600	0.3	47	
(5)	7552-H	648,700	0.3	54	4
(6)	7638-I	525,200	> 6	28	3
(7)	7638-J	455,300	> 8	26	
(8)	7638-K	596,800	> 8	17	
(9)	6360-O	163,400	–	52	
(10)	6360-P	228,200	–	45	
(11)	6360-Q	279,500	–	48	
(12)	7638-R	500,000	> 8	60	
(13)	7638-S	518,000	> 5	60	
	(Natural)				
(14)	7638				
(15)	7638A				
(16)	7638B				
(17)	7552-L	43,500			
(18)	7552-M	43,800			
(19)	7552-N	42,600			

CRD

In an earlier program with 1/8 in. diameter $BaO-UO_2$-W emitters[8] fabricated by BMI, we evolved, in conjunction with BMI, a procedure for fabricating the emitters so that when activated they would yield high fission-fragment flux and thermionic currents. One step in the fabrication process involved mixing and heating $BaCO_3$ with UO_2 whence the carbonate is reduced to BaO, and this step was again duplicated for much of our larger 3/4 in. diameter emitters. However, during the latter part of the present program, BaO was substituted for $BaCO_3$ to simplify the process.

The electron emission from emitters made earlier in this program was low and blisters formed on the surface. After the surface was repolished,

the blisters returned when the emitters were again operated at temperature. CRD
A refinement in the copper sink fixtures employed during the electron beam welding of the emitter to the tantalum tube at Battelle eliminated this blistering problem. With the improved heat sink, the temperature of the emitter surface during the welding cycle fell from white hot to 200°C. Later emitters operated with improved emission but still not as anticipated from the information gathered during the 1/8 in. diameter emitter study program.

It has been concluded, after reviewing the fabrication of the small emit- CRD
ters and the processing prior to emission tests, that there were three major differences in the fabrication and testing of the small and large emitters, viz: (1) $BaCO_3$ was used in all the small emitters; (2) the small emitters were pressed into the small tantalum tubes while all the large emitters required a vacuum seal between the emitter and tantalum tube, thereby necessitating electron beam welding; and (3) the small emitters were baked four to twenty hours at 400°C in a glass UHV system prior to emission tests while the large emitters were operated in a bell jar which was not baked. Because of the complexity of the electron transport tube, the large emitters had to be exposed to air a number of times after heating in a vacuum bell jar which could not be baked out; the emission dropped each time another subassembly was added.

As indicated previously, ETT-5 differed notably from the other diodes U
in that it had a Philips cathode for an emitter, and uranium on molybdenum for the collector. When Philips cathodes for ETT-5 were processed and tested in a manner similar to the $BaO-UO_2$-W emitters, i.e., in an unbaked bell jar and exposed to air between pumping cycles, progressively reduced currents were obtained similar to those from the $BaO-UO_2$-W emitters. For these tests, a special tube with copper gasket and flanges, shown in Fig. 3, was fabricated to contain the emitter and electron-gun subassembly. The tube was baked out at 400°C for 15 hours. The thermionic current density then was approximately normal (10 A/cm^2 at 1100°C). The current did drop however, after the cathode was exposed to air during the final assembly period. It appears that bakeout is important to remove the water vapor before testing the Philips cathode. This should also apply to the $BaO-UO_2$-W emitters since there is some similarity in composition.

U

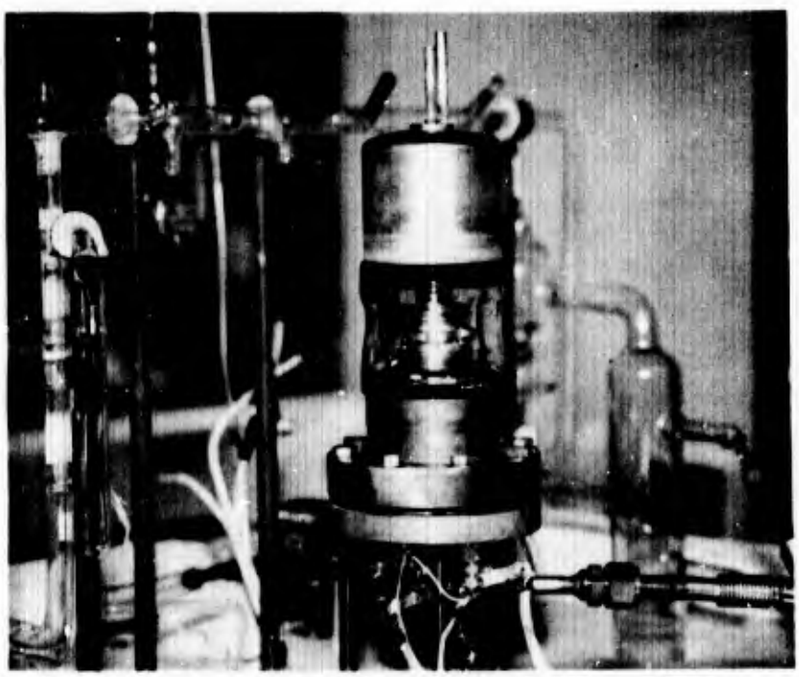

Fig. 3. Bakeable high-vacuum tube for testing Philips cathode and electron-gun subassembly of ETT-5.

We conclude, therefore, that with the encouraging emission results CRD
experienced with the Philips cathodes when they are baked and the similarity between the Philips and the $BaO-UO_2$-W emitters, good emission should also be obtainable from the latter if they (1) are baked, (2) experience temperatures lower than operating temperature during any welding process, (3) are exposed to air a minimum number of times and (4) have $BaCO_3$ rather than BaO in the initial mixing with UO_2.

Usually it is desirable to crimp a Philips emitter onto a base support U
structure. In our case it was necessary to have a vacuum-tight braze joint between the Philips emitter and the tantalum support tube, and this required considerable care to avoid excessive diffusion of nickel onto the emitter surface. Detailed information on the brazing technique is given in the Appendix. Figure 4a shows a photograph of the Philips emitter surface after operating approximately 5 hours at 1100°C as it appeared from the end of ETT-5 transport tube prior to heliarcing the collector. Clearly, nickel from the molybdenum oxide-nickel oxide mixture had diffused through the disc and also had migrated around the edge but no measurable deterioration of emission had occurred at this time.

The molybdenum collector of ETT-5 had a 0.0005 in. thick uranium foil U
nickel brazed to the surface. Detail of this brazing technique is also given in the Appendix. Figure 4b shows a photograph of the collector surface.

Figure 5 shows typical electron transport tube subassemblies U
prior to final assembly. Figures 6a and 6b show some details of the electron gun while Fig. 6c indicates how the tantalum tube containing an emitter is held to the Kovar shell that receives the electron gun. The final tube was processed on a vacuum station as shown in Fig. 6d. Some of the wiring for thermocouples, current, voltage and heating cables along with plumbing for cooling purposes are shown in Figs. 7 and 8a. Figure 8b is a photograph of the equipment for measuring, controlling and monitoring the currents, voltages and coolant flow rates at the reactor.

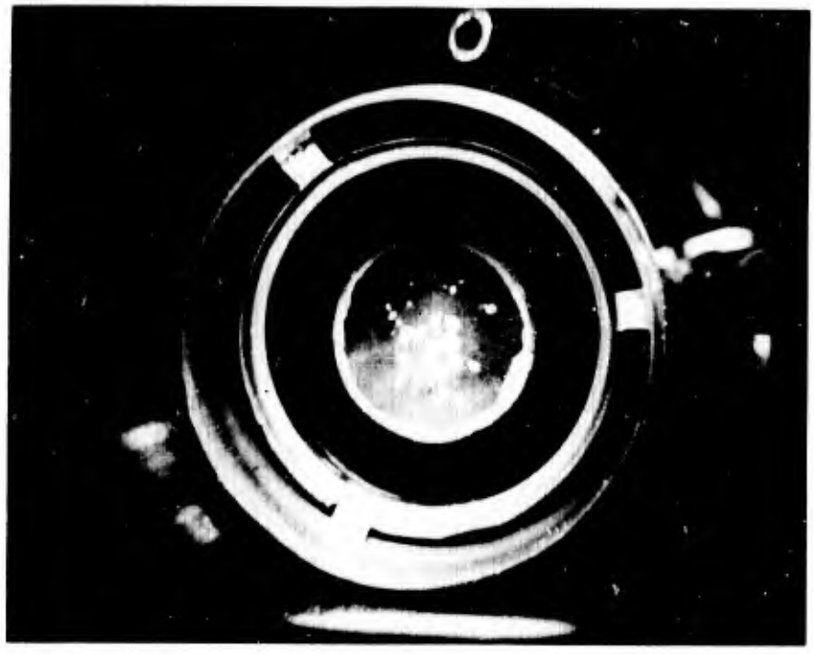

(a)

U

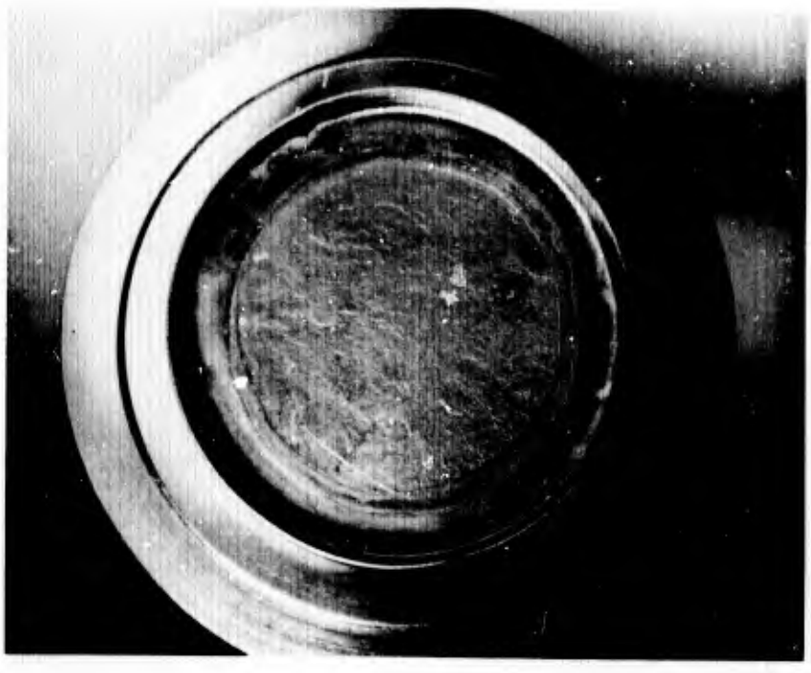

(b)

Fig. 4. Emitter and collector of ETT-5:
(a) Brazed Philips emitter after operating 5 hours at 1100°C;
(b) Uranium foil (0.0005 in.) brazed to molybdenum collector.

Fig. 5. Typical electron transport tube subassemblies.

CRD

(a)

(b)

CRD

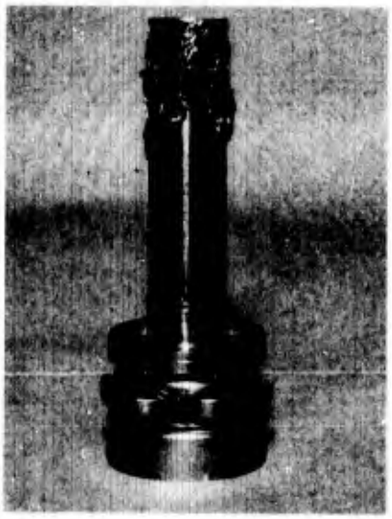

(c)

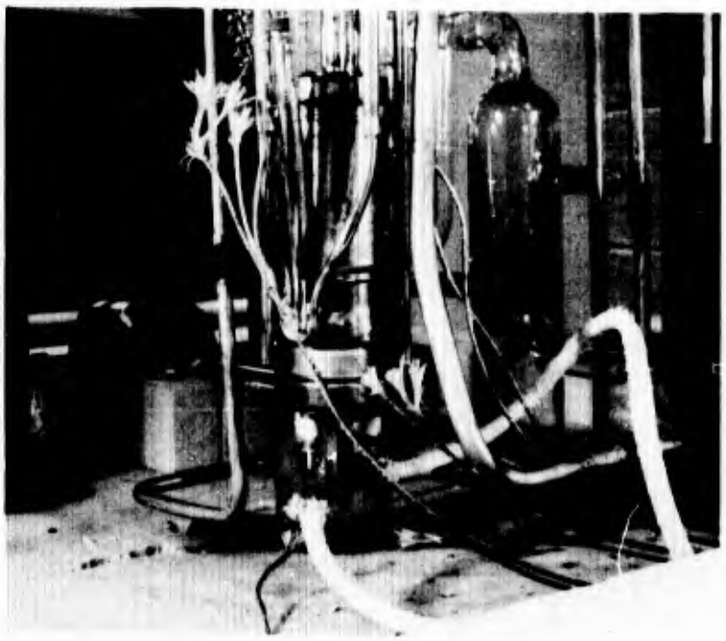

(d)

Fig. 6. (a), (b) Details of electron gun; (c) emitter support structure; (d) final tube processing on high vacuum station.

Fig. 7. Electron transport tube with plumbing and wiring.

U

U

(a)

(b)

Fig. 8. (a) Electron transport tube with all connectors and support structure immediately prior to insertion into 4 ft aluminum containment can.
(b) Measuring equipment for electron transport tube at reactor poolside.

II. 2. Nuclear

Table III shows the results of calculations for determining nuclear parameters which were of interest in this program. The table lists emitter compositions in terms of volume percent (v/o) and mole percent (m/o) loadings, physical dimensions, weight and density of the emitters, thermal neutron cross sections for fission (Σ_f) and absorption (Σ_a), and the neutron self-shielding factor f.

Table III. Calculations of nuclear properties of $BaO-UO_2$-W emitters.

ETT Emitter ETT Tube	7645-D 2	7638-I 3	7552-H 4	6360-0
v/o oxide	76	76	75	63
v/o W	24	24	25	37
m/o BaO	45	38	52	60
m/o UO_2	55	62	48	40
w/o Ba	15.0	14	18.2	16.2
w/o U	35.5	38.2	29.6	19.1
w/o O_2	7.5	7.3	8.3	4.7
w/o W	42.0	40.5	43.9	60.0
Thickness (cm)	0.104	0.071	0.138	0.131
Area (cm^2)	2.55	2.6	2.55	2.57
Volume (cm^3)	0.265	0.185	0.352	0.337
Weight (g)	2.87	1.77	3.82	3.80
Weight - U_{235} (g)	0.95	0.63	1.05	0.68
Ba (g)	0.43	0.25	0.69	0.62
O (g)	0.21	0.13	0.32	0.18
W (g)	1.21	0.72	1.68	2.28
ρ total (g/cm^3)	10.8	9.56	10.8	11.3
ρ U_{235} (g/cm^3)	3.59	3.41	2.99	2.02
ρ oxide (g/cm^3)	8.2	7.46	8.13	7.18
Σ_f (U-235)	5.35	5.08	4.45	3.01
Σ_a (U-235)	6.70	6.41	5.62	3.79
Σ_a (Ba)	0.01	0.01	0.01	0.01
Σ_a (W)	0.28	0.24	0.30	0.42
Σ_a (O)	-	-	-	-
Σ_a (Total)	6.99	6.66	5.93	4.22
f (self shielding)	0.474	0.580	0.426	0.543
P (watts)	210	165	215	165

$\phi = 0.90 \times 10^{13}$ n/cm^2-sec

The total calculated power P(watts) generated in each emitter for a neutron CRD flux of $0.9 \times 10^{13} cm^{-2} sec^{-1}$ is also shown for the emitters employed in diodes ETT 2, 3 and 4. The 6360 emitter represents the type of composition of the two small emitters run inpile during the earlier emitter material study program and reported previously in a classified document.[8] From the plot shown in Fig. 9 of laboratory data of emitter temperature versus input electrical power, we see that about 200 watts is required to heat the emitters in the electron transport tubes to the desired temperature of 1400°C. Table III shows that only the emitters in ETT-2 and 4 were capable of yielding 200 watts of nuclear power and thus meeting the design requirements The 6360 emitter has basically insufficient uranium loading for 1400°C applications. However, in the case of the 7638 emitter of ETT-3 it is not the basic composition that is unsatisfactory; rather the emitter thickness of 0.071 cm is much too small and should be greater than 0.1 cm as with all our other emitters. This unusual thickness deficiency was unfortunately not discovered until ETT-3 was tested inpile when it reached only 1075°C.

Figure 10 shows the effect of emitter thickness on inpile emitter tem- CRD perature, at maximum neutron flux, for the four emitter compositions. These curves are typical of many such thickness calculations carried out for the emitters listed in the previous Table II. It may be noticed that very little is to be gained by thicknesses greater than 0.160 in. This, in a large part, is due to self-shielding. The three data points on the curves represent the inpile experimental data for the three transport tubes.

Figure 11 shows the decrease in α-count as a function of time and number CRD of cycles for each of the three nuclear diode emitters when they were electrically heated to approximately 1400°C. An analysis of the deposit on the collector revealed 90% barium compounds and 10% uranium compounds. Thus, transpiration of uranium from the emitters is not considered the primary cause of the large reduction in α-count at the emitter surface. It appears more likely that an excess of barium was diffusing over the emitter surface and covering the uranium in the emitter.

The thermionic current was also measured at various times in the process- CRD ing of the emitters and these results are shown in Fig. 12. The emitters were exposed to air a number of times in this period and processed in the bell jar at a pressure approximately 5×10^{-7} without bakeout. In all instances the

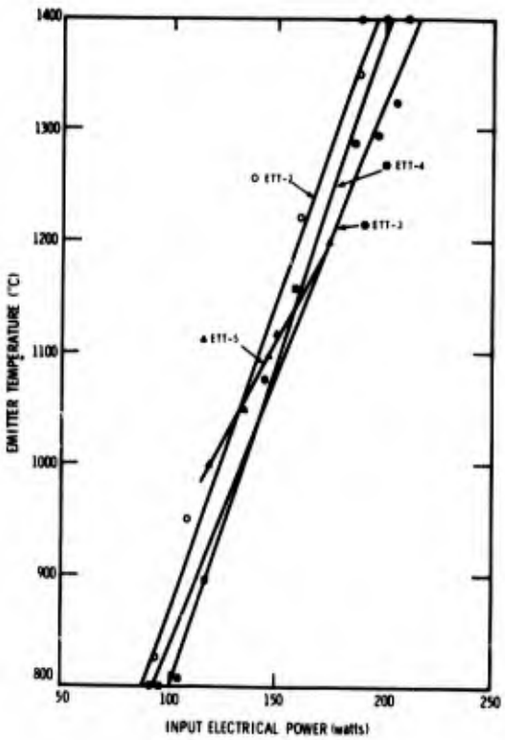

U

Fig. 9. Emitter temperature versus input electrical power.

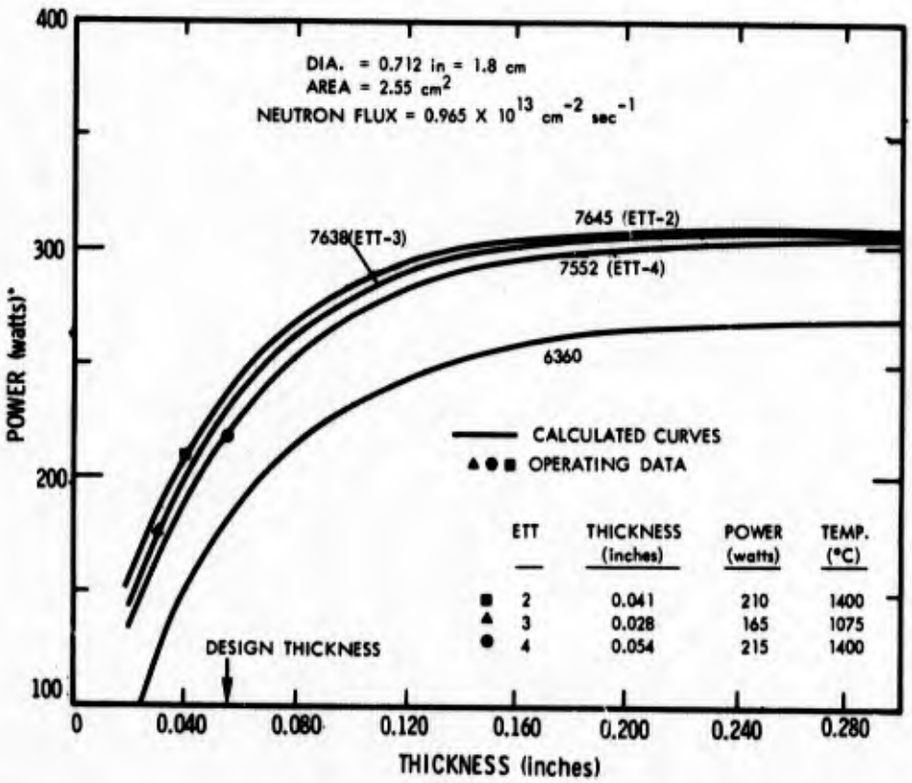

CRD

Fig. 10. Effect of emitter thickness on inpile emitter temperature.

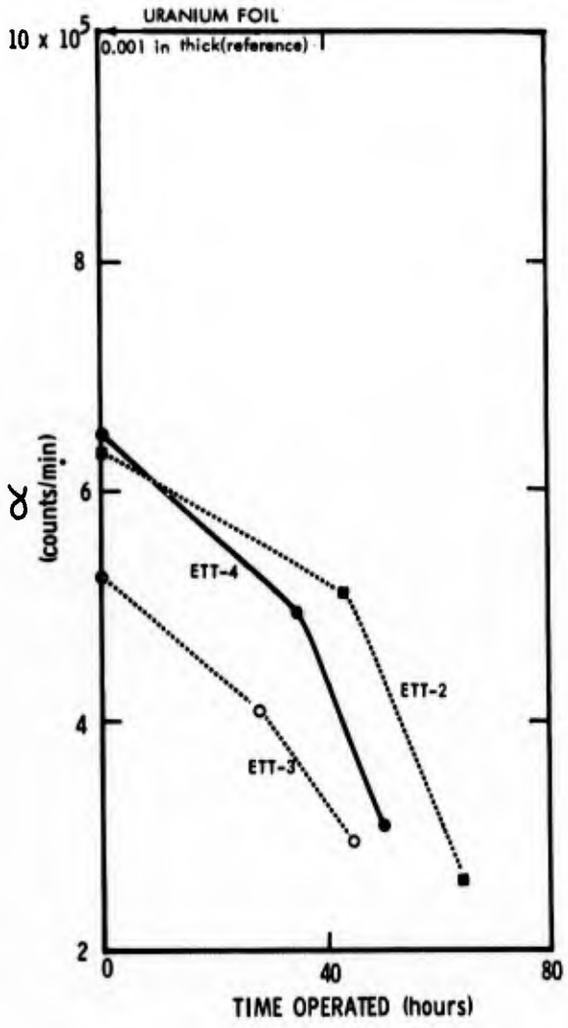

Fig. 11. Decrease in α-particle emission rate as emitter is aged at 1400°C.

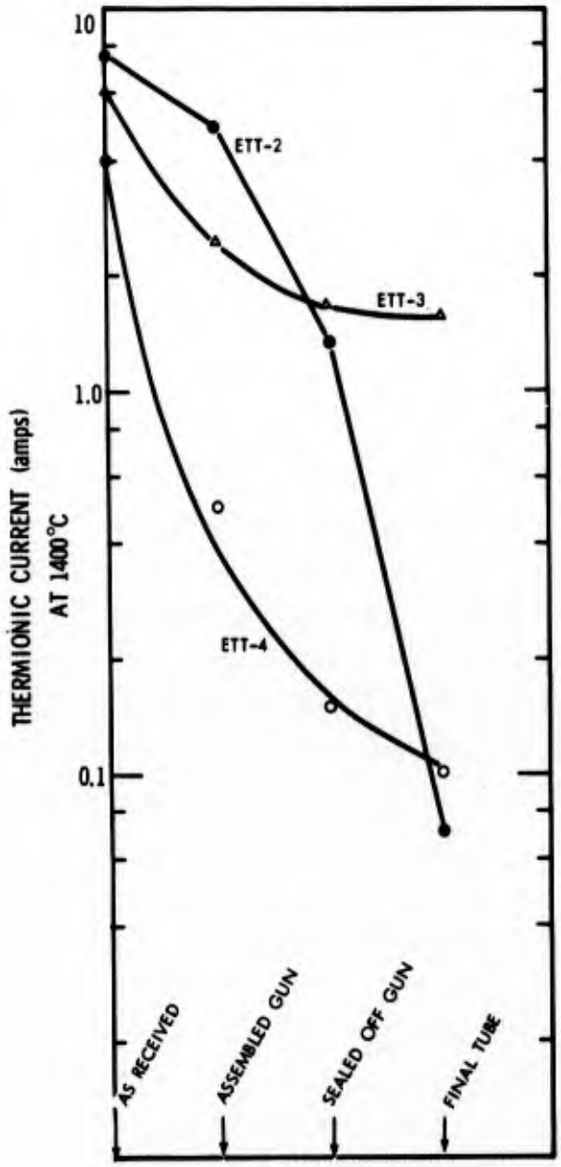

Fig. 12. Effect of air exposure on thermionic emission.

CRD

current continued to decrease along with the α-count for succeeding cycles. Therefore, in order to restrict such emitter deactivation as much as possible, the procedure outlined at the end of Section II.1 should be carefully followed.

II.3. Hot Cell Analysis

Diodes 2 and 3 were examined in the hot cell after they had operated in the reactor until they failed. U

Diode 2 - The first indication of difficulty with Diode 2 was that after 15 megawatt hours the coolant nitrogen gas became radioactive. Analysis conducted in the hot cell indicated that a 1200°C braze joint between the molybdenum disc collector and the connecting stainless steel plenum chamber (Fig.1) had opened; this allowed the fission gases to escape into the nitrogen coolant system. It was known from earlier tests that the collector thermocouple had broken loose from the back of the collector, and so it is quite probable that the indicated thermocouple temperature was less than the true collector temperature by an amount in excess of that which we anticipated. In other words, the collector was probably operating at much too high a temperature. CRD

Both the emitter and collector electrodes appeared to be in satisfactory condition. The emitter appeared slightly gray in color with some minute craters approximately 0.020 in. diam; the collector appeared slightly discolored but there was little evidence of much transpiration of material from the emitter to the collector. CRD

High voltage breakdown occurred in the gun section during the laboratory tests, and as a result, the heater alone was then forced to supply the power to test the emitter at the reduced temperature of 1200°C. (Normally the emitter operates at approximately 925°C with just the heater alone.) However, no damage was observed in the heater or elsewhere in the gun section so that the high voltage breakdown was probably caused by excessive outgassing of air in the gun section. U

Diode 3 - This electron transport tube operated inpile for 8 megawatt hours but never reached the designed temperature of 1400°C. The highest temperature attained at full reactor power was 1075°C. Also, changing the cesium temperature appeared to have no effect on the minute diode current. High voltage breakdown in the gun section during the laboratory test again (as with ETT-2) left only the heater for auxiliary electrical power. Inpile, the CRD

heater appeared to interfere with the emitter thermocouples so that the emitter temperature was uncertain.

Analysis conducted in the hot cell revealed that the tantalum tube containing the emitter at one end had two large elongated holes in it near the electron gun. Further investigation showed that one of the sapphire rods holding the electron gun structure centrally within the tantalum tube (Fig.1) had eroded and allowed the gun to tip and short (or arc) to the tantalum tube and thermocouples. CRD

The opening in the tantalum tube increased the volume of the diode chamber by 30% thereby reducing the overall tube pressure. The fact that the sapphire spacer rod vaporized and the two large holes burned through the tantalum tube, may account for the apparent lack of cesium in the tube since the cesium was then probably converted to an oxide form. CRD

Measurements of the emitter core after destruction in the hot cell revealed the core was only 0.028 in. thick instead of the designed 0.060 in. This lack of thickness in the emitter accounts for the low temperature. Figure 13 shows views of components in Diode 3. It may be noticed in 13a that there is a discoloration on the collector and in 13b the emitter has a central dark ring along with dark regions. Figures 13c and d show the holes burned through the tantalum tube. The α-count from the two diode collectors (i.e., ETT-2 and 3) was approximately three times less than that from the emitter (100-200K counts/min). CRD

II. 4. Electronic

Each of the Diodes 2, 4 and 5 were tested in the laboratory for performance. This included the electron emission characteristics, power input for a given temperature and effect of cesium temperature on the emission. Thermionic current under vacuum conditions was the only laboratory test performed on Diode 3. U

Figure 14 shows the dependence of thermionic current on temperature under vacuum conditions for an applied d.c. voltage pulsed with 20 μsec width pulses and at a repetition rate of 30 pulses per sec. It may be noticed that the emission from ETT-5 is higher than the other diodes. Given the same conditions (i.e. bake, number of cycles, etc.) the emission from the other three $BaO\text{-}UO_2\text{-}W$ emitters should be comparable to ETT-5 (Philips cathode). U

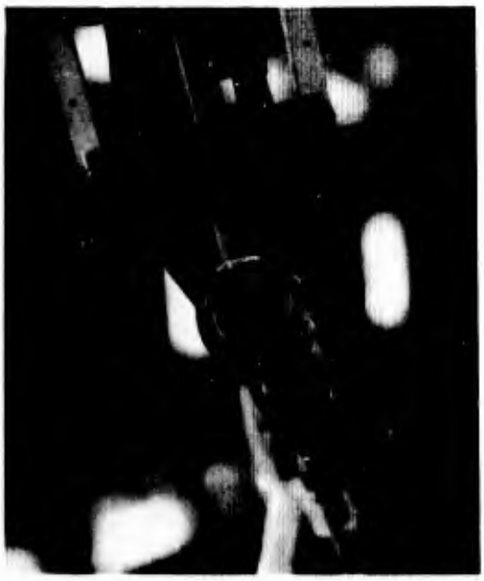

(a)

(b)

CRD

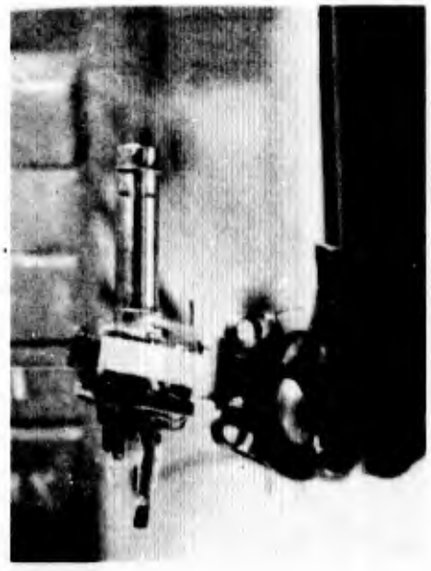

(c)

(d)

Fig. 13. Hot cell disassembly showing components of ETT-3.

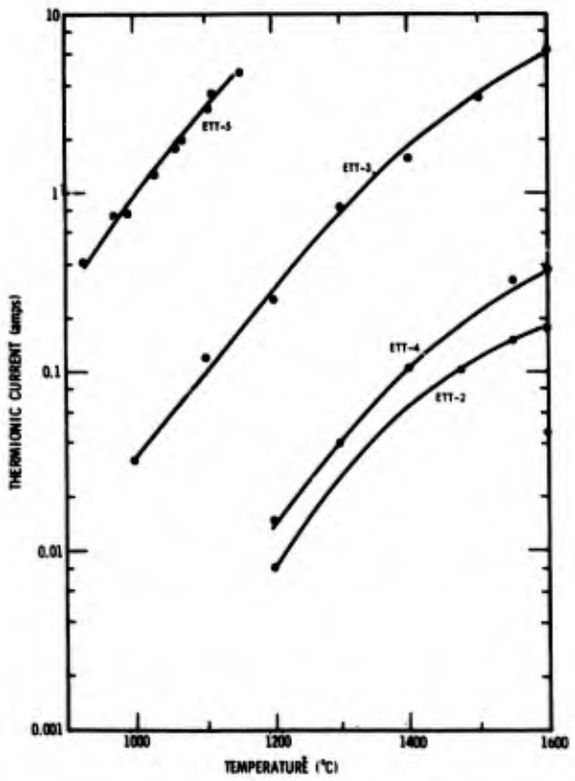

U

Fig. 14. Thermionic Richardson current as a function of emitter temperature.

III. RESULTS

We now discuss consecutively the main results (mostly inpile) obtained with the electron transport tubes. An analysis of these data and comparison with theory are given in Section IV. U

III.1. ETT-2 Inpile and Laboratory Data

Electron transport tube No. 2 was successfully operated inpile and delivered short circuit current of around 1 ampere and greater than 10 amperes at very low positive voltages. In addition, this first inpile run of the transport tube demonstrated that the thermal design of the tube was sound. CRD

This tube operated inpile as a simple diode since the insulator between the jacket and emitter (to null the cesium leakage currents at low tube current) could not be used because of an earlier repair to a leak. In addition the electron gun (to provide an independent heat source for the emitter) failed during processing and the emitter achieved only 1200°C for part of its processing schedule rather than 1400°C; the trouble with the electrical heater was traced to a short circuit between the gun filament and the emitter. The heater operated for a total of 60 hours. CRD

The thermionic emission was relatively poor, 65 mA at 1400°C (Fig. 14), U
as measured by pulse technique under vacuum condition. Figure 15 shows the comparison of the laboratory data between vacuum emission and that for various cesium temperatures with argon present. The vacuum and lowest cesium temperature conditions result in approximately the same current when the vacuum data are extrapolated to zero field. The three cesium curves show that the emission improves as the cesium temperature is increased and the flat portion of the curve indicates some space charge neutralization taking place.

Inpile, this diode achieved a temperature of 1400°C in a neutron flux of $1.26 \times 10^{13} cm^{-2} sec^{-1}$. The cesium cold spot was readily controlled (this had CRD
a heater as well as gas coolant for control) and the other temperatures, such as the ceramic-metal seal, and jacket were well within the tolerance limits. The collector temperature was not as well known as the other temperatures since the thermocouple had pulled off the back surface and was in the gas coolant stream.

In general, at low emitter temperature and thus low electron density CRD
(i.e., low neutron flux region) the open circuit voltage was typically ~ 1.0 volts and the short circuit current was ~ 0.01 amperes. For low positive applied potential (power absorbing quadrant), the net current through the tube frequently increased by sudden jumps as if to indicate various forms of ignited modes. A typical curve is shown in Fig. 16.

As the emitter temperature and electron density were raised however, CRD
(i.e. at higher neutron flux), the current-voltage characteristic did not exhibit these sudden current jumps. Typical curves under these conditions are shown in Fig. 17 where for $Cs/Ar = 5.5 \times 10^{-5}$ the open circuit voltage is 1.5 volts and the short circuit current is 0.9 amperes.

Figure 18 shows the influence of cesium temperature on the emission CRD
with the emitter at a lower temperature (1320°C). There were indications that the temperature of the jacket and collector strongly influenced the emission. There was an enhancement of current experienced inpile compared to that in the laboratory with approximately the same temperature settings.

As indicated earlier, the tube failed after 15 megawatt hours. The braze CRD
joint (nickel-copper) between the back side of the molybdenum collector and the stainless steel plenum opened. This allowed the radioactive gases in the diode to escape into the nitrogen coolant system.

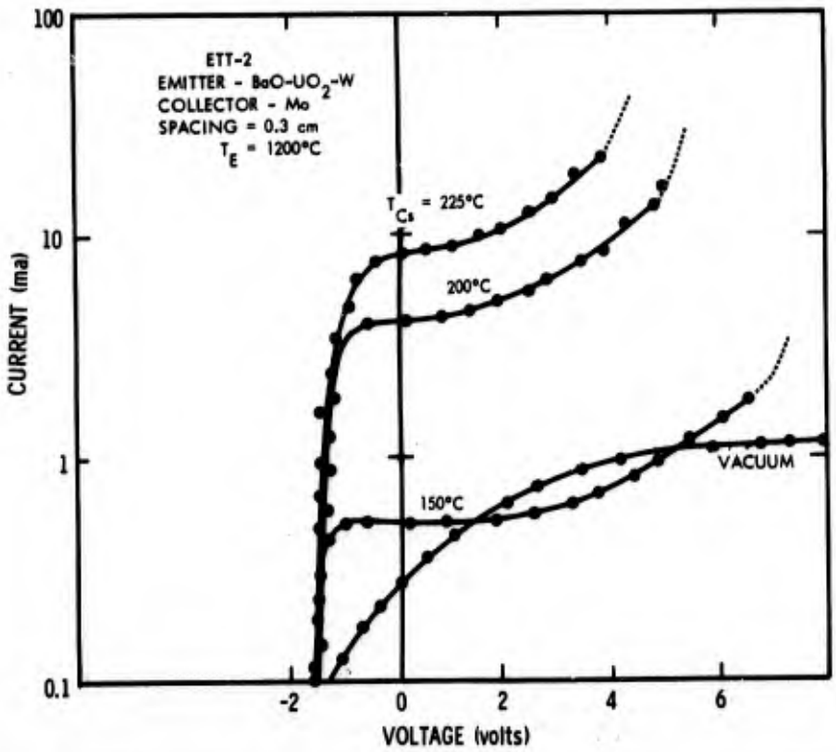

U

Fig. 15. Current-voltage curves for ETT-2 for four laboratory conditions, viz., vacuum, and for an argon density of $3 \times 10^{18} cm^{-3}$ with three cesium bath temperatures of 150°C, 200°C and 225°C.

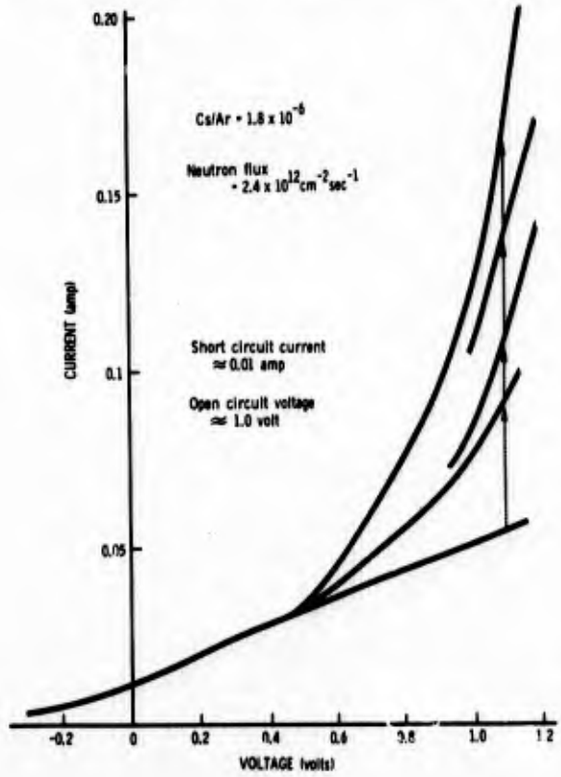

CRD

Fig. 16. Inpile current-voltage curves for ETT-2 for low neutron flux.

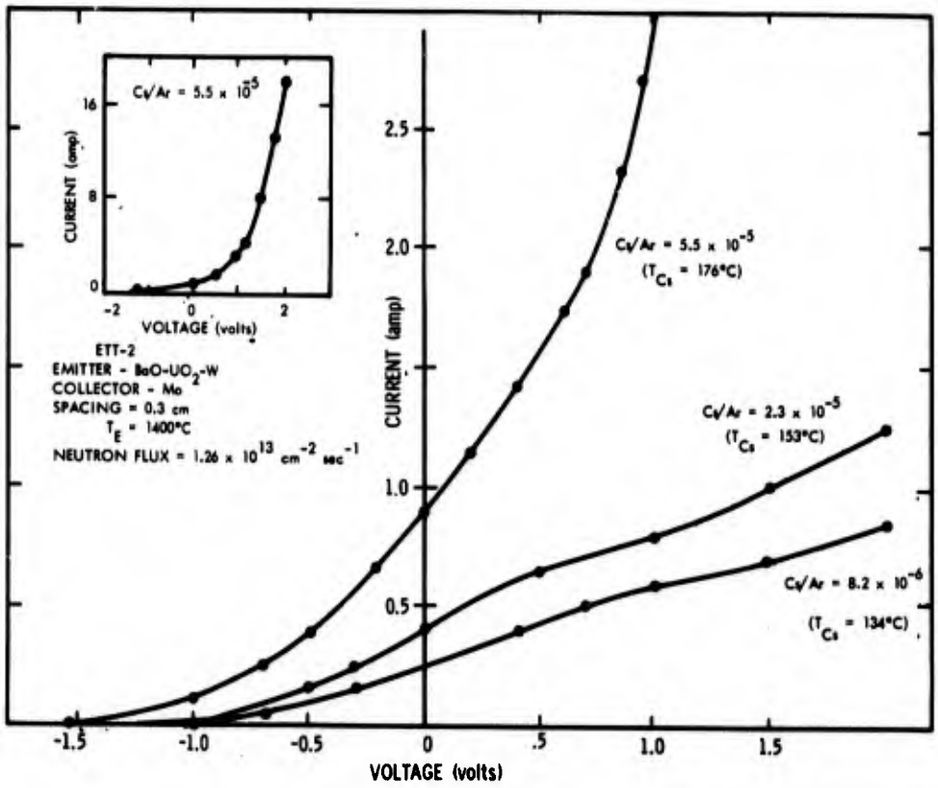

Fig. 17. Inpile current-voltage curves for ETT-2 for high neutron flux.

CRD

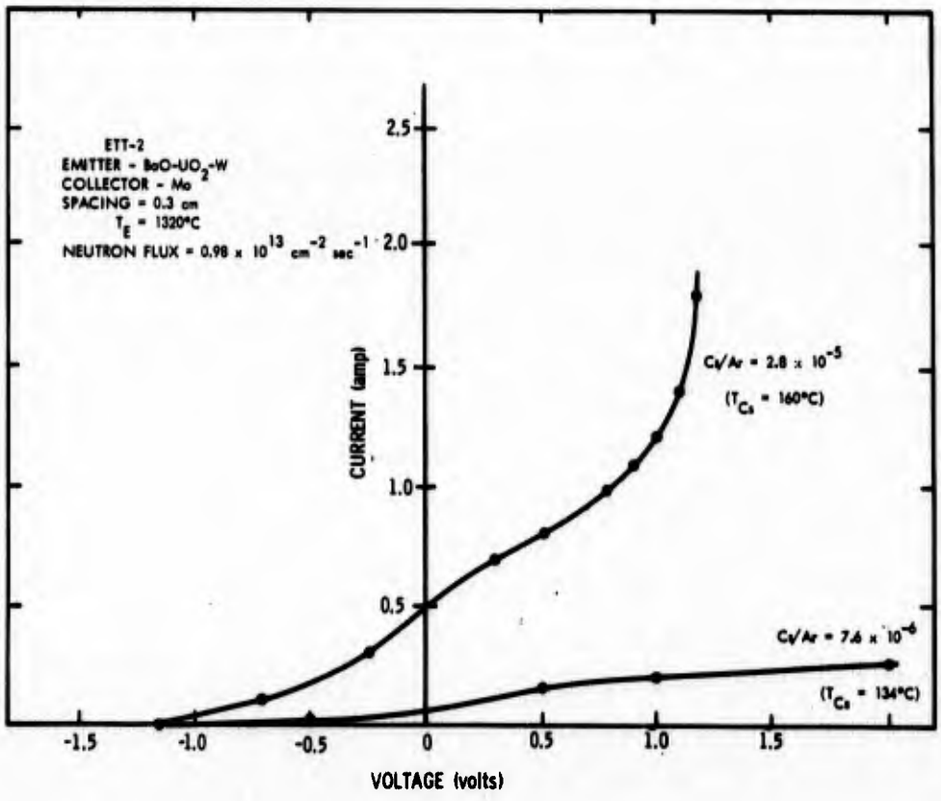

Fig. 18. Inpile current-voltage curves for ETT-2 at reduced emitter temperature.

CRD

III.2. ETT-3 Inpile Data

Electron transport tube No. 3 failed to meet its designed temperature (1400°C) because of insufficient core thickness, (0.028 in. instead of 0.060 in.); the temperature reached was only 1075°C. Also heater power affected the emitter thermocouples making them ineffective. Finally, high voltage breakdown in the gun region, earlier in the laboratory, made it inoperative so that we were unable to use the electron gun to compensate for lack of core thickness. CRD

Structurally, this tube was an improvement over ETT-2. It had a brazed thermocouple on the collector, a stronger gun support and the outer cooling jacket served as a third electrode for cesium leakage current control. CRD

Laboratory data were purposely not taken in order to keep the emitter free of cesium until going inpile where we could study the effect of cesium on the emitter. The pulsed emission data (Fig. 14) indicate the emitter was the best of the three $BaO\text{-}UO_2$-W emitters incorporated into diodes. U

Inpile, there were indications of a leaky tube since the current was only milliamperes with either positive or negative voltage, and also the emission was insensitive to changes in cesium temperature. Thus, after only 8 megawatt-hrs. of operation, the tube was examined in the hot cell. The result of this examination has already been discussed in Section II.3 and shown in Fig. 13. CRD

III.3. ETT-4 Inpile and Laboratory Data

Electron transport tube No. 4 was successfully operated inpile at the design temperature and delivered short circuit current of about 0.9 ampere and greater than 30 amperes at very low positive voltages. Maximum power output was 0.2 watts and the tube operated for 50 MW hrs. Initially the tube had a floating jacket but electrical leakage developed across the emitter-to-jacket insulator restricting the tube behavior to a simple diode. High voltage breakdown in the gun region again prevented full use of the gun, although the heater alone was operative for most of the inpile studies. Fabrication improvements over ETT-3 included improved insulation in the gun region and larger cooling capabilities for the cesium reservoir; the proper thickness for the emitter core was obtained with this tube. CRD

The pulsed emission data of Fig. 14 show that the current was only slightly greater than for ETT-2. Laboratory data comparing vacuum emission with that in an argon-cesium atmosphere are shown in Fig. 19. Again, as in ETT-2, the projected short circuit current under vacuum and low cesium bath temperature U

condition agree well. The current always returned to the original value when the cesium bath temperature was increased to 200°C and then decreased to room temperature; this indicates there is no permanent activation of the emitter. The high ion current shown in Fig. 19 for 200°C cesium bath temperature is not understood. Under certain temperature conditions, spurious currents both in the positive and negative direction with respect to the emitter were often observed with short circuit currents as high as 0.5 A.

Figure 20 shows inpile current data as the cesium temperature was varied when the emitter was at 1375°C. Figure 21 also shows the variation of inpile current data due to changes in cesium temperature when the emitter was at CRD 1400°C and the temperatures of the other components was held constant. Note that the short circuit current is lower than in Fig. 20 due mainly to the different collector and jacket temperatures. The family of curves in Fig. 21 for the different cesium temperatures do not follow the same pronounced trend as was noticed for ETT-2 in Fig. 17. We see from Fig. 21 that over a large range of Cs/Ar values (10^{-6} to 10^{-3}) the current-voltage curves do not differ markedly.

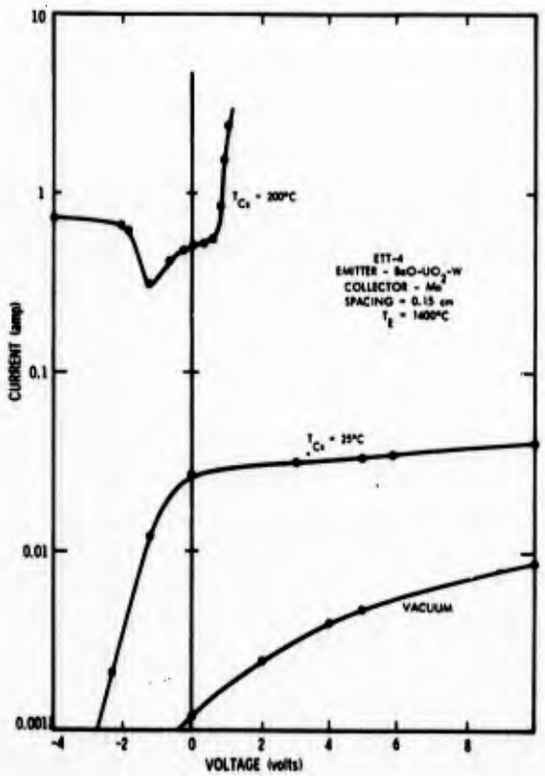

U

Fig. 19. Current-voltage curves for ETT-4 for three laboratory conditions, viz., vacuum and for an argon density of $3 \times 10^{18} cm^{-3}$ with two cesium bath temperatures of 25°C and 200°C.

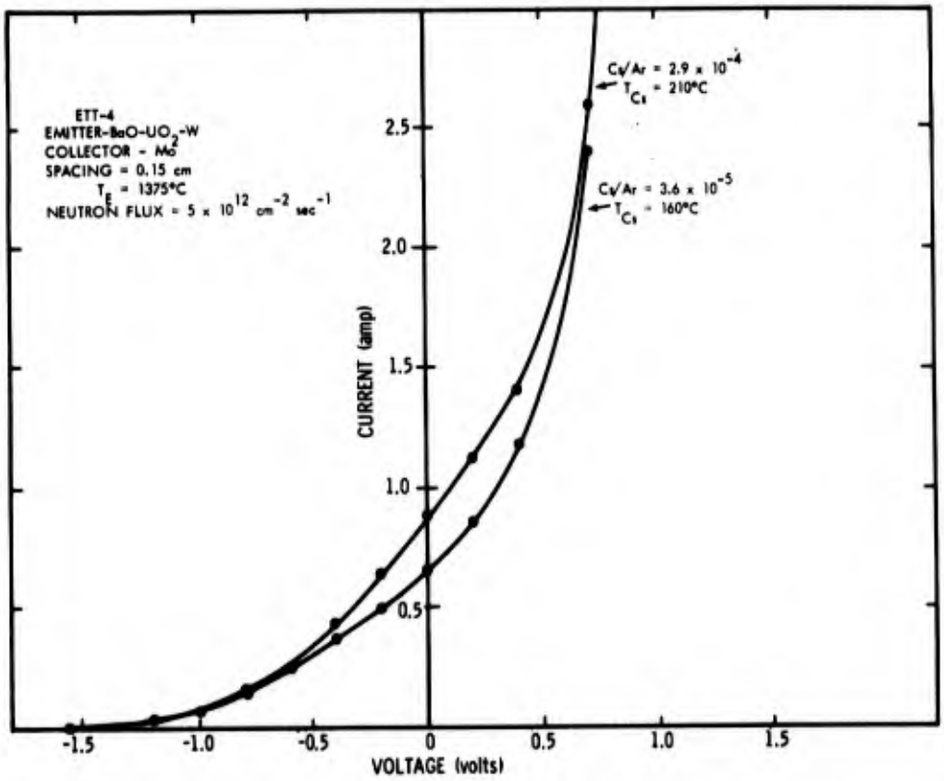

CRD

Fig. 20. Inpile current-voltage curves for ETT-4 at emitter temperature of 1375°C.

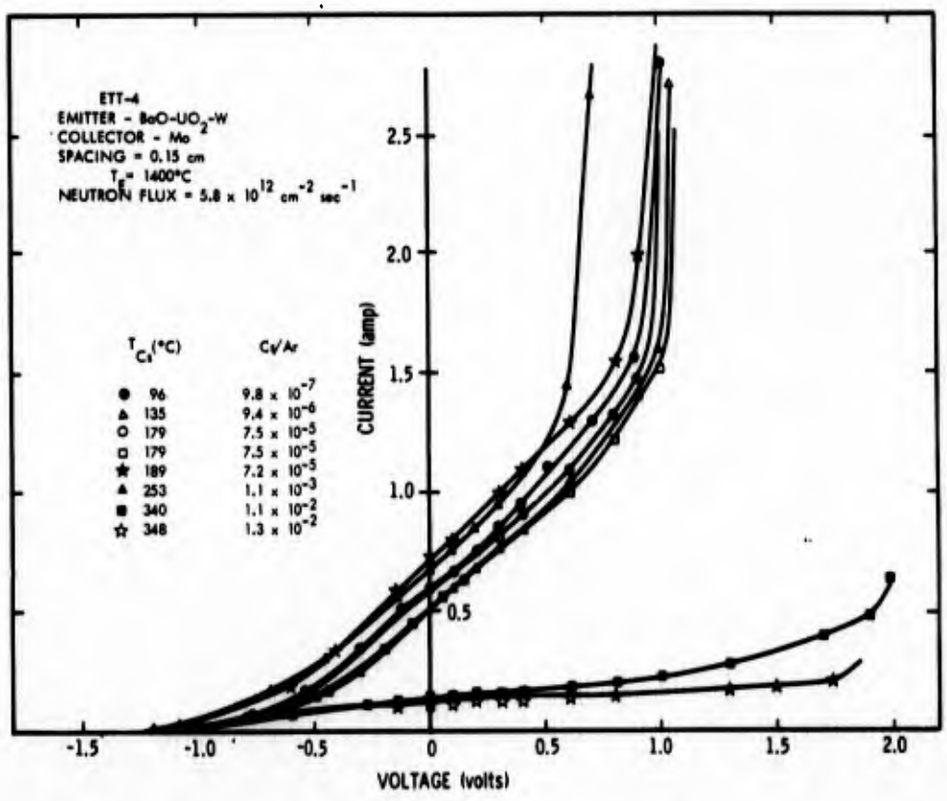

CRD

Fig. 21. Inpile current-voltage curves for ETT-4 showing the dependence of current on Cs/Ar ratio (i.e. cesium bath temperature) keeping the temperature of all other components carefully constant.

A cleaner presentation of these data is given in Fig. 22 where the 8 short circuit current values in Fig. 21 are plotted against the Cs/Ar ratio. CRD The short circuit current remains quite constant for Cs/Ar$<10^{-3}$ and then shows a strong decrease over the highest range studied (10^{-3} to 10^{-2}).

The maximum current studied was 30 amperes at approximately 2.2 volts. CRD No conclusive results were obtained to correlate the current with neutron flux since the emitter temperature could not be kept constant over a wide-enough region of neutron flux. This was due to lack of high voltage capabilities in the electron gun.

It is emphasized that in both ETT-2 and ETT-4 the current was very sensitive to temperature variations of the emitter, collector, jacket and cesium cold spot. Other than the cesium temperature, the jacket temperature appeared to CRD have the most influence on the current. It is not clear from the transport tube data whether a surface effect or gas reaction kinetics accounts for this electron current variation with jacket temperatures. This point is discussed further in Section IV.

The ETT-4 tube continued to operate until the Delrin insulator disc sealing the top of the four foot aluminum containment can developed numerous cracks CRD and shrank due to the high neutron flux. This allowed pool water to enter the evacuated 4 ft tube and corrode the transport tube.

III.4. ETT-5 Laboratory Data

Electron transport tube No. 5 with the Philips cathode and uranium-on-molybdenum collector had a good electron gun throughout the laboratory tests. U Other than the emitter and collector, only minor changes were made over ETT-4.

Pulsed vacuum emission (Fig. 14) indicated this emitter was the best of any in the four tubes. Laboratory data with the emitter at 1100°C are shown in U Fig. 23. Under vacuum conditions, and for an argon filling at the cesium bath temperatures of 112°C and 185°C, the currents are well-behaved (in contrast to some of the laboratory data at 200°C obtained with ETT-4 shown in Fig. 19). It was thus anticipated that with ETT-5 operating at emitter temperatures significantly lower than in our previous electron transport tubes, the complete influence of fission fragment ionization could be more clearly ascertained. Unfortunately, the copper pinch-off region of the diode developed a leak after pinch-off and the diode was thus ruined before obtaining any inpile data. This was the last tube of the program.

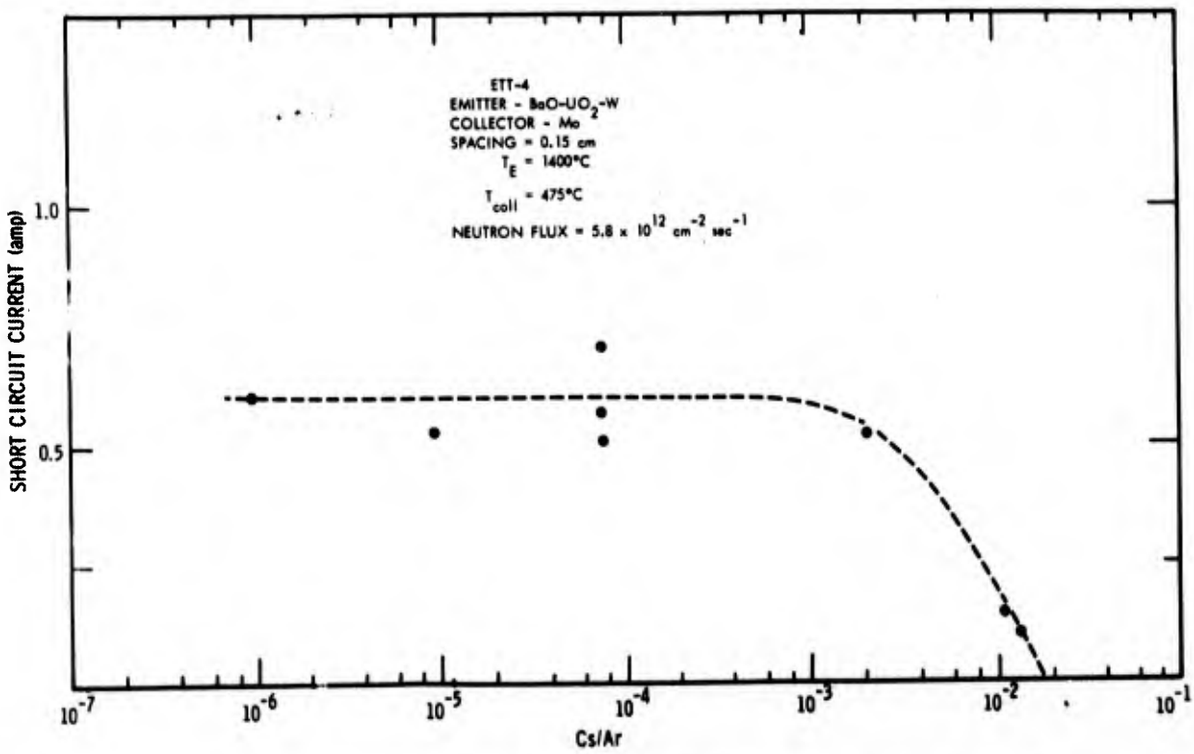

CRD

Fig. 22. Short circuit current for ETT-4 as a function of Cs/Ar ratio.

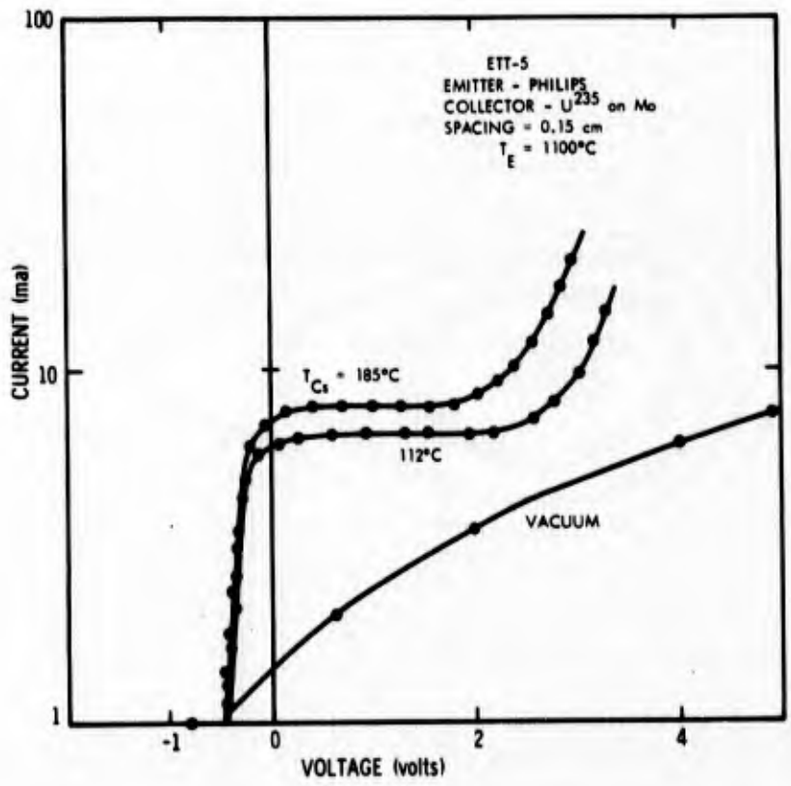

U

Fig. 23. Current-voltage curves for ETT-5 for three laboratory conditions of vacuum, and argon-filled with cesium bath temperatures of 112°C and 185°C.

IV. ANALYSIS OF INPILE ELECTRON-TRANSPORT DATA

We have developed two approaches to the conductivity of a fission-fragment induced noble gas plasma. Our first theory was concerned with the reaction kinetics at a point in such a plasma[1] and, although it did account for the overall diffusion loss of ions, the resultant number was the electron density at the center of the tube. This approach was appropriate for the analysis of our microwave data and in particular for those effects that depend upon an average of the number density over the volume of the cavity. However, this theory is not sufficient to predict details of electron transport, that is, to predict the current-voltage characteristics of a thermionic converter, since these characteristics depend upon the properties of the plasma at the boundaries as well as at the center of the tube. In particular, we can expect that the plasma properties very near the collector surface will be important. U

For our second approach to electron transport in a noble-gas plasma we set up as a goal the solution of the differential equations for the electron transport at each point across the plasma. The boundary conditions for the plasma would be the sheath characteristics at the emitter and collector surfaces. With the complex reactions occurring in the plasma as described by our reaction kinetics theory, a solution of the complete set of equations would be analytically intractable and very difficult numerically with a computer. We decided to attack this problem in two steps; first, to develop a diffusion transport solution where the volume recombination loss of the dominant ion is ignored,* and secondly, to solve numerically with a digital computer a somewhat simplified version of the differential transport equations in which all of the various volume recombination loss processes were represented by a number of terms in various powers of the electron density. U

We have presented the theory[2] and the AS9 computer code[1] for electron transport in a diffusion controlled plasma in previous reports. From this model the shape of predicted I-V characteristics were consistent with earlier U

* The important recombination loss of the ion of the major gas — which is Ar_2^+ in the case of the Ar-Cs system — is taken into account in the diffusion transport model by calculating the effective value of $W(eV/_{ip})$ for fission fragments in the presence of dissociative recombination of Ar_2^+ which in turn leads to the production of Ar^m metastable states capable of ionizing cesium. U

laboratory and inpile measurements. However, it became clear that even though high electron densities were predicted for the center of the tube ($\sim 10^{12} cm^{-3}$) for typical conditions in the University of Michigan research reactor, the important electron density at the collector was very much lower ($\sim 3x10^{10} cm^{-3}$). In this typical example the random electron current in the plasma at the collector surface ($J_e = e\, n_e \bar{v}_e/4$) became controlling and yielded very low values for the diode current density (80 mA/cm^2) even with an emitter capable of $J_r = 2.0\ A/cm^2$. The predictions of this pure diffusion theory were quite discouraging for the potential of a thermionic converter using neon-argon ionized by fission fragments. Furthermore, one cannot expect a higher predicted current density when volume recombination losses are added to the model; rather, these additional ion losses would be expected to lower the electron density at the collector even further.

Nevertheless, a numerical solution of the differential transport equations including recombination terms was attempted in the AW6 computer code. U This code does successfully solve the differential equations consistent with the boundary conditions and yields the electron density distribution across the plasma. However the last part of the code where the electric field is integrated across the plasma to give the electrode potential difference in terms of the electron current, has not yet been completed. The reader is reminded again that the trend will likely be to lower the predicted current-voltage characteristics when the volume recombination losses are included.

From our reaction kinetics studies, the argon-cesium system appeared to be appreciably better than the neon-argon system not only because higher ($\sim x2$) U center-of-tube electron densities were predicted but also because the electron scattering cross section for argon is much less than for neon so that argon should give a lower electron-neutral atom resistivity. As discussed earlier in this report, we filled our electron transport tubes with argon ($\sim$100 torr) and attached a cesium bath in order to vary Cs/Ar.

In this section we will compare the current-voltage curves from the AS9 U code for the diffusion-controlled transport theory with selected experimental curves from the inpile runs for both the ETT-2 and ETT-4 tubes.

IV. 1. Fission and Ion Generation Rates for ETT-2

This tube had a spacing of 0.3 cm and a $BaO-UO_2$-W fuel of designation 7645-D as described in Sections II.2 and III.1. From the composition of the fuel, the macroscopic fission cross section was computed to be $\Sigma_f = 5.35$, cm^2 as noted earlier in Table III. The computed nuclear heat generation rate of 196 watts for $\phi = 1.45 \times 10^{13} cm^{-2} sec^{-1}$ agreed well with the laboratory measured value of 197 watts at $T_E = 1400°C$. The fission power density in the fuel from neutrons entering from one side (j) of the fuel disc is given by CRD

$$\dot{E}\ (\text{watts cm}^{-2}) = \left(\frac{P}{A}\right) = \left(\frac{\Sigma_f}{\Sigma_T}\right)\ \left(\frac{\phi_o}{4}\right)\ \left(\frac{f_j}{3.1 \times 10^{10}}\right)\left[e^{-(\overline{\Sigma_a d})}\right]_j ,$$

where f_j is the fraction of neutrons entering from one side, Σ_T is the total macroscopic fission cross section, ϕ_o is the unperturbed neutron flux and $\phi = \left[\phi_o e^{-(\overline{\Sigma_a d})}\right]$ is the neutron flux attenuated by the tube structure except for the fuel. It is this last value ϕ that we measure with our gold foil activation techniques in a mockup assembly (and by our flux probe). $\dot{E} = \dot{E}_1 + \dot{E}_2$ is the total fission power from neutrons entering from both sides. Later when we compute the fission rate at the top surface it will be important to distinguish between the neutron currents from above and below.

The fission rate in the volume of the fuel (of thickness t and area A) from neutrons from one direction is CRD

$$\left(\frac{\dot{F}}{At}\right)_j \left(\frac{\text{fiss sec}^{-1}}{\text{cm}^3}\right) = \left(\frac{\Sigma_f \phi}{2}\right)_j \left(e^{-(\overline{\Sigma_a d})}\right)_j$$

where ϕ is described above and now the exponential factor corrects mainly for the fuel itself. For neutrons from both sides we have

$$\left(\frac{\dot{F}}{At}\right) = \tilde{\Sigma}_f \phi$$

where $$\tilde{\Sigma}_f = \left(\frac{e^{-(\overline{\Sigma_a d})}\ \text{Top} + e^{-(\overline{\Sigma_a d})}\ \text{Bot.}}{2}\right) \Sigma_f ,$$

and for this fuel we obtain $\tilde{\Sigma}_f = \left(\frac{0.815+0.12}{2}\right) 5.35 = 2.50\ cm^{-1}$. It is immediately evident that the fission rate at the surface of this emitter has been

reduced from that for our thin uranium foils (microwave and ion generation rate tubes) where $\tilde{\Sigma}_f$=21.7 cm^{-1}.

For Cs/Ar=5.5x10^{-5} (see Fig. 17) we computed an eV/ion pair, corresponding to just the Cs^+ ion production, of ω_α=28.3 eV/ion pair. With this ω_α value and a $\tilde{\Sigma}_f$=2.50 cm^{-1}, an ion generation rate code run (Q00 91.7) was made for p=110 torr and ϕ=1.35x$10^{13}cm^{-2}sec^{-1}$ to give S^+_{mid}=0.371x$10^{16}cm^{-3}sec^{-1}$. This value of source rate was used as input to the AS9 diffusion code with J_{RICH}=2.5 A/cm^2. The predicted I-V curve from the AS9 code displayed in Fig. 24 is much lower than the experimental curve. This discrepancy between theory and experiment is discussed below in Section IV.3. CRD

IV. 2. Fission and Ion Generation Rates for ETT-4

We decided to narrow the gap of this tube to 0.15 cm as compared to 0.30 cm for ETT-2. This would certainly lower the predicted I-V curve from the diffusion model and give us further evidence of its validity. This tube also used a somewhat different fissile fuel composition (7552-H) for the emitter (Σ_f=4.46 cm^{-1}). A calculation similar to that for the ETT-2 fuel gave $\tilde{\Sigma}_f$=2.05 cm^{-1}. CRD

The inpile run chosen for comparing the diffusion theory with experiment had a neutron flux of ϕ=7.58x$10^{12}cm^{-2}sec^{-1}$. The Q00 code gave S^+_{mid}=0.144x$10^{16}cm^{-3}sec^{-1}$. Using this as input to the AS9 diffusion code (Run 42.0) with J_{RICH}=0.70 A/cm^2 gave the computed curve of Fig. 25 which again can be seen to be very much lower than the experimental curve. CRD

IV. 3. Discussion of Fit of Theory with Experiment

We turn now to a brief discussion of possible reasons why the inpile short-circuit currents found in ETT-2 and ETT-4 are much higher than expected. It is interesting to note that these elevated current data are in line with some of our previous unexplained microwave cavity results of electron density versus gas temperature. In our last report[1] (unclassified) we presented a curve (Fig. 11, page 16) of the logarithm of electron density versus the reciprocal gas temperature which exhibited (on those scales) a linear temperature dependence far more severe than we could account for from our reaction kinetics predictions. (We recall that the predictions of our reaction kinetics theory were in excellent agreement with all the experimental results for the case of neon with traces of argon). The range of gas temperature CRD

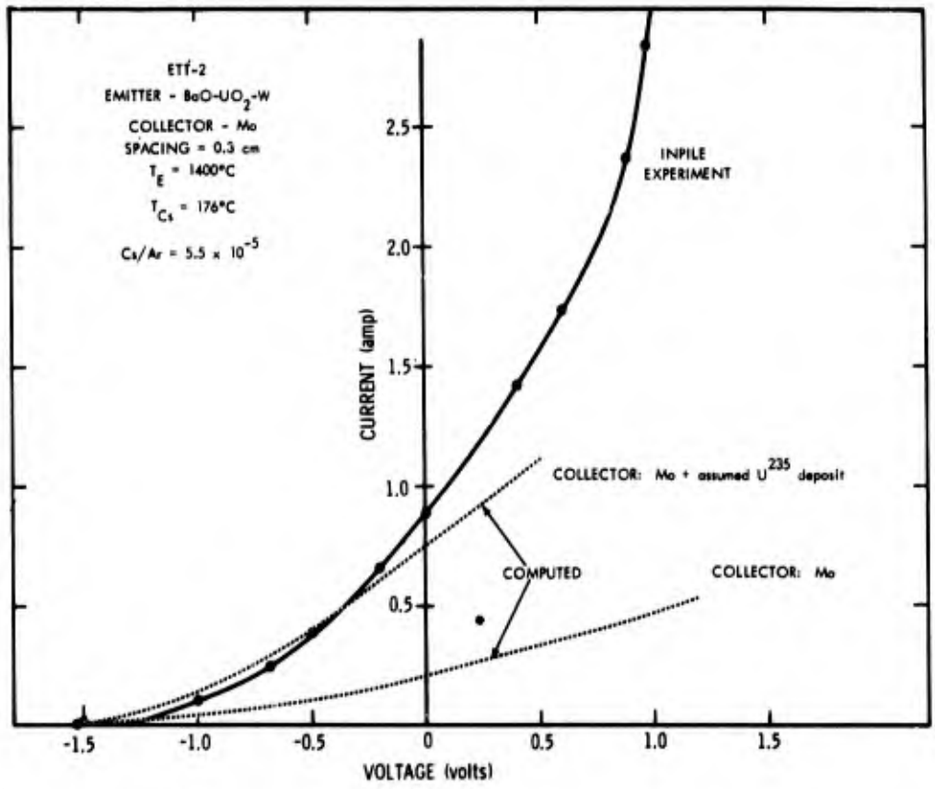

CRD

Fig. 24. Comparison of inpile experimental I-V data for ETT-2 with predictions of the diffusion-loss dominated thermioric transport model.

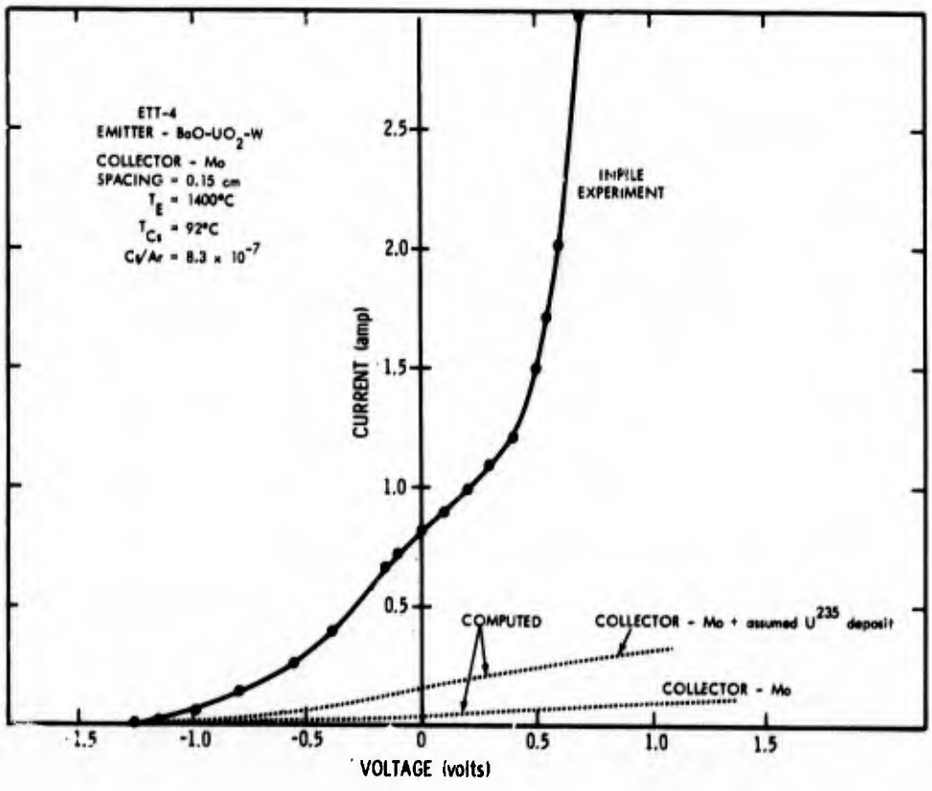

CRD

Fig. 25. Comparison of inpile experimental I-V data for ETT-4 with predictions of the diffusion-loss dominated thermionic transport model.

covered experimentally in the Ar-Cs microwave experiments was limited to 400-700°K; however, if this curve is extrapolated up to the gas temperatures (~1300°K) typical of ETT-2 and ETT-4, then the value of electron density becomes about $10^{13}cm^{-3}$ (an order of magnitude greater than predicted) which is more in accord with the electron density required to account for the electron transport data. Thus for Ar-Cs there exists a consistency between the experimental microwave data and the experimental electron transport tube data.

With regard to Figs. 24 and 25 we emphasize that the diffusion theory does not account for recombination loss of the dominant Cs^+ ions in the volume of the plasma and should therefore predict a diode current higher than that for our actual conditions where appreciable recombination losses are indicated. Yet, the experimental currents (I_E) are much higher than the diffusion theory current predictions (I_T) for both the ETT-2 tube ($I_E/I_T \sim 5$) and the ETT-4 tube ($I_E/I_T \sim 30$). In fact, the experimental data appear to be independent of diffusion losses since the short circuit current for the ETT-4 tube with d=0.15 cm, was essentially the same as that for the ETT-2 tube with d=0.30 cm. In an effort to explain this behavior, the following topics (indicated by subheadings) were explored. CRD

(a) Uranium Deposit on Collector - After the ETT-2 data were taken, we wondered if some of the uranium-235 was somehow transferred to the collector surface thus providing a higher fission fragment yield and thence a higher ion generation rate. A computer code run was made assuming a full range thickness of U-235 on the collector surface ($5x10^{-4}cm$) together with a non-depleted emitter surface. This curve (dashed) is shown in Fig. 24 where we see that the predicted short circuit current is now much closer to the measured value. However, a similar calculation for the ETT-4 did not improve the fit very much (Fig. 25) indicating that U-235 transfer was not the cause. Also the ETT-2 tube was dismantled in a hot cell after the inpile runs (Section II.3) and there was essentially no measure of U-235 on the collector (as determined by α-counter). CRD

(b) Surface Ionization of Cesium by Thermal Contact - The $BaO-UO_2$-W emitter was enclosed in a tantalum cup which in turn was welded to the tantalum support can (Section II.1). We considered the possibility that cesium might be ionized on a portion of this hot, high work function, tantalum support surface and that the ions then migrate into the interelectrode gap. Our computations indicated that surface ionization of cesium was most unlikely to account for the CRD

increased electron current. Nevertheless, as a precautionary measure, our final electron transport tube ETT-5 was designed to operate at an emitter temperature 200-300°C lower than our other tubes so that the high current effect could be absolutely isolated from any possible conventional thermal contact-ionization of cesium.

(c) Surface Ionization of Cesium by Collisions of the Second Kind - In our fission fragment generated plasmas many energetic particles are lost from the plasma by diffusion to the walls. In the case of pure noble gases most of this energy is lost non-productively and the small production of secondary electrons on the pure metal walls can be neglected. In the case of argon-cesium, however, the collector has cesium atoms adsorbed on the surface. All of the energetic argon species Ar^+, Ar_2^+, Ar^m and Ar^* which are diffusing to the wall have ample energy to ionize a cesium atom. Unfortunately, very little can be found in the literature on the interaction of a plasma with cesium adsorbed on a surface. From the critical importance of the electron density in the vicinity of the collector we can say that any increase in ion generation rate at the collector surface from such collisions of the second kind would have a very pronounced effect on the electron transport properties. U

Although we could not compute this additional source of ions, we nevertheless wanted to make an estimate of the upper limit of such an effect to see if it could account for the higher measured current. To make this computation we reasoned as follows: If the energetic particles diffusing to the walls created both a cesium ion and an electron in collisions with cesium atoms at the walls then the total ion (or electron) distribution could be approximated by the assumption of no ion loss by ambipolar diffusion. For the computation, we in fact set all diffusion loss rates equal to zero which implies one Cs^+ ion produced for each Ar^+ and Ar_2^+ ion striking the walls, no wall losses of Ar^m and the equivalent of complete reflection of each cesium ion. All ions must therefore be lost by volume recombination. We do not expect this much wall production of ions but we consider that this must certainly be an upper bound. We can now use our reaction kinetics codes, set all diffusion constants equal to zero and obtain a value for the electron density. This normally would have given only the value at the center of the tube but with this present no-diffusion transport model, it also gives the value of the electron density at the collector ($\tilde{n}_{ec}$); we can then compute $\tilde{J}_{max}=\tilde{n}_{ec}\,\bar{v}/4$ as the upper bound for the transport current. Computations were CRD

made for the conditions of the ETT-4 run in Fig. 25 except that the gas pressure was varied; the results are shown in Fig. 26. This curve (3a) for n_e vs p peaks at a lower pressure (p~35 torr) than for the gas filling pressure of ~100 torr for ETT-4. The electron density distribution from emitter to collector at 100 torr for all three models are also depicted in Fig. 26. The pure diffusion theory (3b) has the highest center of tube value of n_e but a very low value of electron density at the collector n_{ec} such that $I_{ec}=J_{ec}A_c=A_c n_{ec}\bar{v}/4=0.03$ A. By including recombination the center of the tube value drops to $n_{ec} \simeq 0.4\times10^{12}cm^{-3}$ (1b) and the value at the collector is expected to be even lower than for the pure diffusion model. On the other hand, the pure recombination model (curves (3a) and (3b)) gives a value at 100 torr of $\tilde{n}_{ec}\simeq 1.2\times10^{12}cm^{-3}$ and $\tilde{J}_{max}\simeq 2.5$ A. This is certainly higher than the measured short circuit current of 0.9 A. We can conclude only that the proposed wall source of cesium ions is not inconsistent with the experimental data and further experimentation would be needed.

(d) Electron Transport Tube ETT-5 - In order to further test this wall-source model we decided to build a special diagnostic tube designed to maximize the fission fragment ion generation rate in order to see if the transport current scaled properly with ion generation. Since we had not obtained full activation of our $BaO-UO_2$-W emitters in the laboratory we decided to construct this tube with a standard Philips emitter and put a thin uranium film on the collector as discussed in Sections II.1 and III.4. Furthermore, operating with an emitter temperature as low as 1200°C insured that tantalum support structures could in no way contribute any significant thermal contact ionization of cesium. We completed construction of this tube but the pinch-off seal failed during laboratory testing.*

The results of the computations for this tube are shown in Fig. 26 as the upper set of curves. Because both the thin uranium film on the collector and the Philips emitter are essentially transparent to neutrons, the ion generation rate is increased a factor of 4.75 over that for the equivalent ETT-4 run. As shown the predicted short circuit current would be increased a factor of 10/2.5=4 over that for the ETT-4 run. It can also be seen by comparing the two curves of n_e vs p for the recombination loss only model (3a and 4a) that the maximum electron density has been shifted to a higher pressure (~60 torr).

* Sufficient time was not available to construct a second tube before termination of the project.

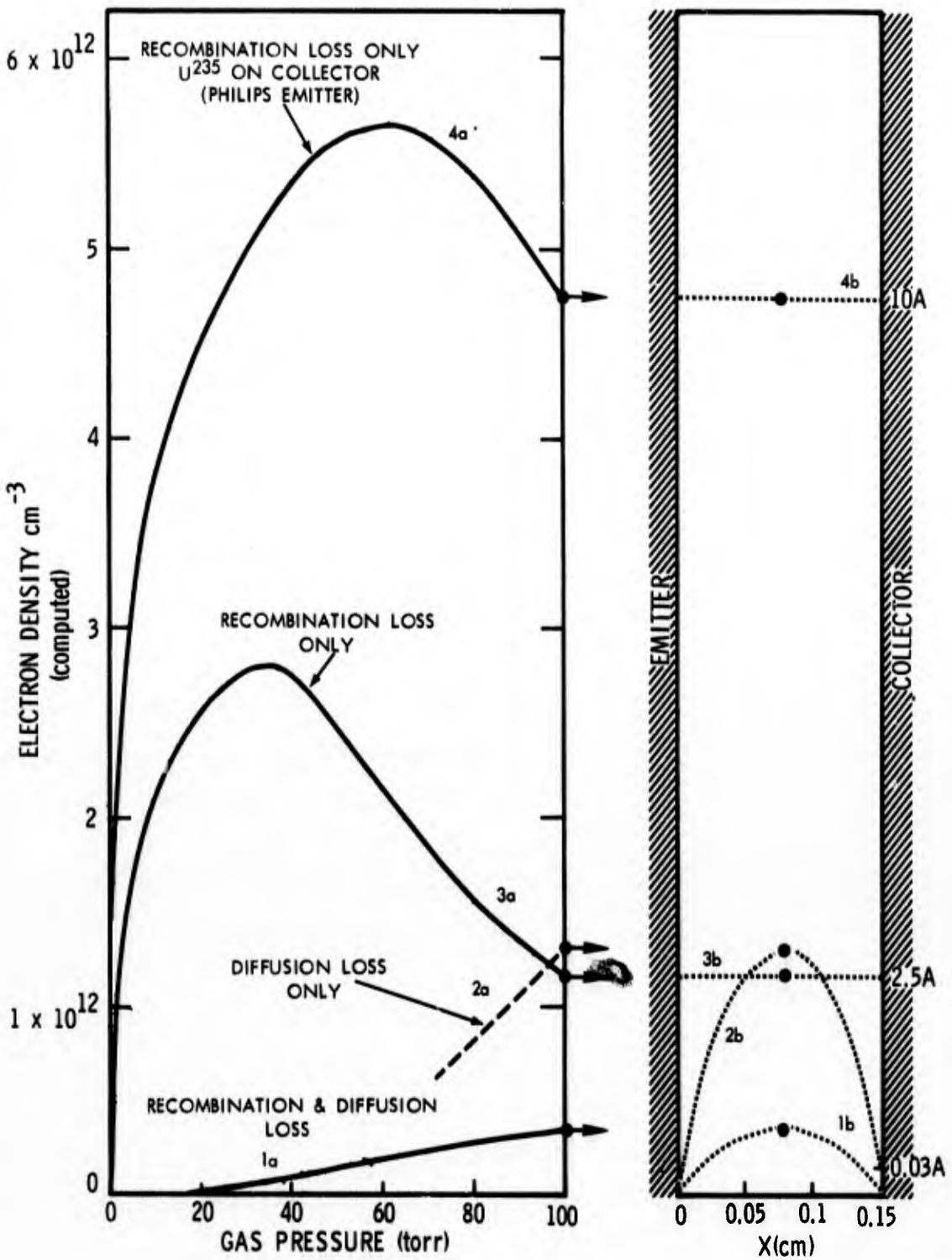

CRD

Fig. 26. Computed electron density versus gas pressure, and electron density distribution across diode for three models of (1) Recombination and Diffusion Loss, (2) Diffusion Loss only, and (3) Recombination Loss only.

Had we been able to run this tube inpile and obtained a factor of 4 increase in short circuit current (i.e. 4x0.9=3.6 A) then we would have established at least that the unknown additional ion source did scale with ion generation rate. This tube, by itself, could probably not produce sufficient data to establish the mechanism for increased ion production but it would certainly have been a major step in that direction. CRD

ACKNOWLEDGMENTS

This work was performed under the direct supervision of Dr. Frank E. Jamerson: his encouragement, interest and guidance throughout these studies are gratefully acknowledged. The authors also wish to thank Professor David J. Rose of the Massachusetts Institute of Technology for many stimulating and enlightening discussions on plasmas. Invaluable technical assistance in the design and fabrication of the tubes and inpile test systems was given by Messrs R. J. Dusman, R. M. Aikin, D. M. Lee, and their contributions throughout the program are gratefully recognized. Thanks are also expressed to the University of Michigan reactor staff for their ready cooperation and help during the inpile experiments. U

REFERENCES

U

1. C. B. Leffert and D. B. Rees, ONR Annual Report No. 7, Contract Nonr-3109(00), AD 806 963, (Oct. 1966).
2. C. B. Leffert, D. B. Rees, and F. E. Gifford, ONR Annual Report No. 6, Contract Nonr-3109(00), AD 475 633, (Oct. 1965).
3. C. B. Leffert, D. B. Rees, and F. E. Jamerson, ONR Annual Report No. 5, Contract Nonr-3109(00), AD 609 177, (Oct. 1964).
4. C. B. Leffert, F. E. Jamerson, and D. B. Rees, ONR Annual Report No. 4, Contract Nonr-3109(00), AD 425 231,(Oct. 1963).
5. F. E. Jamerson, et al., ONR Annual Report No. 3, Contract Nonr-3109(00), AD 290 727,(Oct. 1962).
6. F. E. Jamerson, et al., ONR Annual Report No. 2, Contract Nonr-3109(00), AD 273 062, (Jan. 1962).
7. D. H. Loughridge, et al., ONR Annual Report No. 1, Contract Nonr-3109(00), AD 250 673, (Dec. 1960).
8. F. E. Gifford and R. F. Hill, ONR Final Report, Part I(Unclassified) and Part II(Classified), Contract Nonr-3870(00), (July, 1964).

APPENDIX

1. Heat Losses in Electron Transport Tube

Below are the results of calculations to determine the heat losses in the transport tube. These losses account for the approximately 200 watts of input power required to heat the emitter to 1400°C. U

A) Conduction

1)	Leads to gun structure	3 W
2)	Tantalum support tube for the emitter	30 W
3)	Ar-Cs gas near the emitter surface and approximately 1/2 in. down the tantalum tube where the temperature is visible	15 W
B)	Radiation	150 W

The input power for all the tubes was shown in Fig. 9. Figure 2 showed the variation of the temperature of the principal components with emitter temperature. U

2. Recirculating System

The collector, jacket and cesium reservoir were cooled to desired temperatures by recirculating nitrogen gas through the three systems. Separate controls for each system permitted individual selection of proper heat balance on each side of the insulators and firm control of the cesium reservoir temperature. The cesium reservoir could also be separately heated by a.c. power to an insulated nichrome wire wound around the reservoir. Protective devices were included in the nitrogen system to switch to tank nitrogen in case of electrical power failure or pump difficulty. A flow diagram of the entire recirculating system is shown in Fig. 27. U

3. Emitter and Collector Braze for ETT-5

The 0.715 in. diameter x 0.062 in. thick Philips cathode disc was brazed at 1375°C in the end of the tantalum tube with a mixture of 53.5% Ni and 46.5% Mo fine powder in amyl acetate. One of the tantalum tubes containing natural uranium was modified for the Philips cathode by removing the $BaO-UO_2-W$ core. This allowed the Philips cathode to be brazed on the back side to the tantalum end section. The tantalum surface was prepared by nickel plating followed by vacuum firing to 1450°C to outgas and melt the nickel. The Philips U

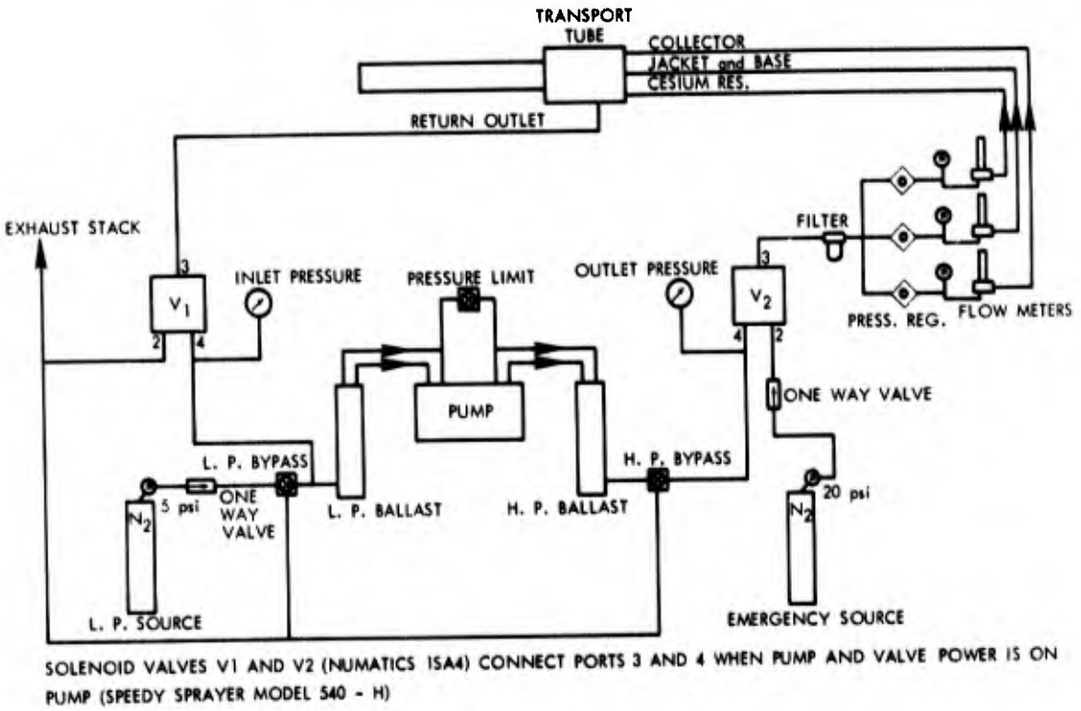

Fig. 27. Cooling-gas recirculating system.

cathode was flashed with nickel but not fired. The emitter surface was protected by masking with cellulose during the plating operation. A thick coating of Mo-Ni mixture was applied to the nickel plated back surface of the emitter to about 1/16 in. from the edge. The noncoated surface was to discourage the nickel from migrating across the 0.062 in. thickness and onto the emitting surface during testing. Under vacuum condition the weighted emitter disc was brazed to the nickel coated tantalum at 1375°C. The temperature was brought to approximately 1200°C for ten seconds and quickly raised to 1375 for only a few seconds. The braze was deemed completed when the temperature of the emitter surface suddenly turned from spotty condition to a uniform temperature. During the emission testing later, it was noticed that bright spots appeared on the surface and a bright rim on the periphery of the surface. Further testing caused the spots and rim to grow. Later analysis by x-ray technique showed the bright areas to be nickel. Figure 4a showed a photo of this emitter.

Uranium was nickel brazed to the molybdenum collector. A nickel flash was first melted onto the molybdenum surface followed by another approximately 2 mil thick of nickel plating. After the last nickel coat was outgassed at 1200°C in vacuum, a 0.001 in. thick uranium foil was held flat on the molybdenum collector by a quartz disc and heated in vacuum. The braze was effective at about 1100°C. Figure 4b showed a photo of the uranium on molybdenum collector. The uranium foil was etched to 0.005 in. thickness in full strength HNO_3 in approximately 45 minutes.

UNCLASSIFIED CONFIDENTIAL RESTRICTED DATA

Security Classification

DOCUMENT CONTROL DATA - R&D

(Security classification of title, body of abstract and indexing annotation must be entered when the overall report is classified)

1. ORIGINATING ACTIVITY (Corporate author)
Research Laboratories, General Motors Corporation
12 Mile and Mound Roads, Warren, Michigan 48090

2a. REPORT SECURITY CLASSIFICATION
Confidential Restricted Data

2b. GROUP

3. REPORT TITLE
INVESTIGATIONS ON THE DIRECT CONVERSION OF NUCLEAR FISSION ENERGY TO ELECTRICAL ENERGY IN A PLASMA DIODE.

4. DESCRIPTIVE NOTES (Type of report and inclusive dates)
Volume II of Final Report No. 8 - November 1, 1966 to October 31, 1967

5. AUTHOR(S) (Last name, first name, initial)
Gifford, Fay E.
Leffert, Charles B.
Rees, David B.

6. REPORT DATE	7a. TOTAL NO. OF PAGES	7b. NO. OF REFS
October 31, 1967	58	8

8a. CONTRACT OR GRANT NO.	9a. ORIGINATOR'S REPORT NUMBER(S)
Nonr-3190(00)	GMR Item No. 2731
b. PROJECT NO. 099-345	
c.	9b. OTHER REPORT NO(S) (Any other numbers that may be assigned this report)
d.	None

10. AVAILABILITY/LIMITATION NOTICES
Qualified requesters may obtain copies of this report from DDC.

11. SUPPLEMENTARY NOTES	12. SPONSORING MILITARY ACTIVITY
None	Office of Naval Research Power Branch (Code 429) Dept. of the Navy, Washington, D.C. 20360

13. ABSTRACT

This is the classified section (Vol.II) of the Final Report under Contract Nonr-3109(00), Office of Naval Research, dealing with fission-fragment-generated plasmas for thermionic energy conversion. Inpile experiments on the transport of thermionic electrons through the argon-cesium plasma are described and the results are compared with predictions of a diffusion-loss dominated transport model and recombination-dominated limits. The inpile experiments were performed using ceramic-metal diodes of parallel-plane configuration filled to a pressure $p(Ar) \approx 100$ torr and $10^{-6} \lesssim Cs/Ar \lesssim 10^{-2}$, with an unclad thermionic-electron and fission-fragment emitter($BaO-UO_2-W$), and also containing an evacuated electron-gun section by means of which the emitter temperature could be heated in a manner independent of the nuclear heat. Maximum short-circuit current densities of about 0.3 A cm^{-2} were obtained in these diagnostic diodes at a neutron flux value of around $1 \times 10^{13} cm^{-2} sec^{-1}$. These current densities were much higher (by factors of 5 to 30) than those predicted by the diffusion-loss dominated transport-model. Furthermore, in marked contrast with theory, these current densities were similar for two values of emitter-collector spacing (0.15 and 0.3 cm). This makes the present system appear more attractive for practical thermionic applications than can be expected on the basis of simple transport-models. Quantitative recombination-dominated limits suggest that the experimental findings are more consistent with a uniform emitter-collector electron density profile. As a result, it is tentatively suggested that the incidence of excited and charged argon species upon cesium-covered metal surfaces gives rise to a wall source of both ions and electrons which in effect significantly reduces the expected ambipolar diffusion loss of charge from the plasma.

DD FORM 1 JAN 64 1473

UNCLASSIFIED CONFIDENTIAL RESTRICTED DATA

Security Classification

14. KEY WORDS	LINK A		LINK B		LINK C	
	ROLE	WT	ROLE	WT	ROLE	WT
1. Direct energy conversion 2. Thermionics 3. Gaseous electronics 4. Plasma physics						

INSTRUCTIONS

1. ORIGINATING ACTIVITY: Enter the name and address of the contractor, subcontractor, grantee, Department of Defense activity or other organization *(corporate author)* issuing the report.

2a. REPORT SECURITY CLASSIFICATION: Enter the overall security classification of the report. Indicate whether "Restricted Data" is included. Marking is to be in accordance with appropriate security regulations.

2b. GROUP: Automatic downgrading is specified in DoD Directive 5200.10 and Armed Forces Industrial Manual. Enter the group number. Also, when applicable, show that optional markings have been used for Group 3 and Group 4 as authorized.

3. REPORT TITLE: Enter the complete report title in all capital letters. Titles in all cases should be unclassified. If a meaningful title cannot be selected without classification, show title classification in all capitals in parenthesis immediately following the title.

4. DESCRIPTIVE NOTES: If appropriate, enter the type of report, e.g., interim, progress, summary, annual, or final. Give the inclusive dates when a specific reporting period is covered.

5. AUTHOR(S): Enter the name(s) of author(s) as shown on or in the report. Enter last name, first name, middle initial. If military, show rank and branch of service. The name of the principal author is an absolute minimum requirement.

6. REPORT DATE: Enter the date of the report as day, month, year; or month, year. If more than one date appears on the report, use date of publication.

7a. TOTAL NUMBER OF PAGES: The total page count should follow normal pagination procedures, i.e., enter the number of pages containing information.

7b. NUMBER OF REFERENCES: Enter the total number of references cited in the report.

8a. CONTRACT OR GRANT NUMBER: If appropriate, enter the applicable number of the contract or grant under which the report was written.

8b, 8c, & 8d. PROJECT NUMBER: Enter the appropriate military department identification, such as project number, subproject number, system numbers, task number, etc.

9a. ORIGINATOR'S REPORT NUMBER(S): Enter the official report number by which the document will be identified and controlled by the originating activity. This number must be unique to this report.

9b. OTHER REPORT NUMBER(S): If the report has been assigned any other report numbers *(either by the originator or by the sponsor)*, also enter this number(s).

10. AVAILABILITY/LIMITATION NOTICES: Enter any limitations on further dissemination of the report, other than those imposed by security classification, using standard statements such as:

(1) "Qualified requesters may obtain copies of this report from DDC."

(2) "Foreign announcement and dissemination of this report by DDC is not authorized."

(3) "U. S. Government agencies may obtain copies of this report directly from DDC. Other qualified DDC users shall request through _____."

(4) "U. S. military agencies may obtain copies of this report directly from DDC. Other qualified users shall request through _____."

(5) "All distribution of this report is controlled. Qualified DDC users shall request through _____."

If the report has been furnished to the Office of Technical Services, Department of Commerce, for sale to the public, indicate this fact and enter the price, if known.

11. SUPPLEMENTARY NOTES: Use for additional explanatory notes.

12. SPONSORING MILITARY ACTIVITY: Enter the name of the departmental project office or laboratory sponsoring *(paying for)* the research and development. Include address.

13. ABSTRACT: Enter an abstract giving a brief and factual summary of the document indicative of the report, even though it may also appear elsewhere in the body of the technical report. If additional space is required, a continuation sheet shall be attached.

It is highly desirable that the abstract of classified reports be unclassified. Each paragraph of the abstract shall end with an indication of the military security classification of the information in the paragraph, represented as *(TS)*, *(S)*, *(C)*, or *(U)*.

There is no limitation on the length of the abstract. However, the suggested length is from 150 to 225 words.

14. KEY WORDS: Key words are technically meaningful terms or short phrases that characterize a report and may be used as index entries for cataloging the report. Key words must be selected so that no security classification is required. Identifiers, such as equipment model designation, trade name, military project code name, geographic location, may be used as key words but will be followed by an indication of technical context. The assignment of links, rules, and weights is optional.